

# 九岭地区东槽细晶岩型铌钽矿床年代学、 岩石地球化学特征及其地质意义

党飞鹏<sup>1</sup>, 吕川<sup>1</sup>, 张勇<sup>2</sup>, 肖志斌<sup>3</sup>, 张涛<sup>1</sup>, 陈欣<sup>1</sup>, 李志鹏<sup>1</sup>,  
汤君阳<sup>1</sup>, 罗建群<sup>1</sup>

(1. 核工业二七〇研究所, 江西 南昌 330200; 2. 东华理工大学核资源与环境国家重点实验室, 江西 南昌 330013;  
3. 深层油气全国重点实验室 中国石油大学(华东), 山东 青岛 266580)

**摘要:** 近些年在赣西北九岭地区南部新预测了潭山-上富 Nb-Ta-Li-Be 成矿远景区, 成矿类型包括花岗岩型和细晶岩型两类, 对其进行形成时代和成因机制的研究是认识九岭地区铌、钽、锂等稀有金属富集成矿的关键。对东槽矿床含铌钽细晶岩开展了铌铁矿族矿物 U-Pb 年代学、岩相学和岩石地球化学研究, 确定了其成岩成矿年龄、岩石成因和源区特征, 并浅析其成矿潜力。结果显示, 铌钽铁矿 LA-ICP-MS U-Pb 年龄为  $142 \pm 1$  Ma, 表明含铌钽细晶岩的成岩、成矿时代均在燕山早期(早白垩世)。含铌钽细晶岩以斜长细晶岩为主, 具有富硅、富碱、富铝、低钛、贫稀土元素、Rb/Sr 值变化大, 富集铌、钽、锂、铷以及  $\text{CaO}/(\text{K}_2\text{O}+\text{Na}_2\text{O}) \leq 0.10$ 、 $\text{Al}_2\text{O}_3/\text{TiO}_2 > 160$  和高的分异指数( $\text{DI} \geq 90$ )等特征, 其稀土元素配分曲线呈弱右倾“海鸥型”, 微量元素蛛网图左侧隆起和右侧平缓, 表明该细晶岩与强过铝质高分异 S 型花岗岩特征相似。综合分析认为, 东槽细晶岩是九岭地区新元古界双桥山群变泥质岩在构造应力场由挤压向伸展演变的背景下发生部分熔融, 并经历高程度结晶分异演化的产物。东槽含铌钽细晶岩与南岭含铌钽花岗岩、大湖塘含铌钽花岗斑岩具有相似的地球化学特征, 铌、钽、锂等元素含量高, 是潭山-上富成矿远景区重要的成矿地质体。

**关键词:** 铌钽矿床; 细晶岩; 地球化学; 铌钽铁矿 U-Pb 年龄; 九岭地区

中图分类号: P618.79; P618.86

文献标识码: A

文章编号: 1000-6524(2024)04-0938-18

## Geochronological and petrogeochemical characteristics of Dongcao aplite-type niobium-tantalum deposit in Jiuling area and their geological significance

DANG Fei-peng<sup>1</sup>, LÜ Chuan<sup>1</sup>, ZHANG Yong<sup>2</sup>, XIAO Zhi-bin<sup>3</sup>, ZHANG Tao<sup>1</sup>, CHEN Xin<sup>1</sup>,  
LI Zhi-peng<sup>1</sup>, TANG Jun-yang<sup>1</sup> and LUO Jian-qun<sup>1</sup>

(1. Research Institute No. 270, CNNC, Nanchang 330200, China; 2. State Key Laboratory of Nuclear Resources and Environment, East China University of Technology, Nanchang 330013, China; 3. State Key Laboratory of Deep Oil and Gas, China University of Petroleum (East China), Qingdao 266580, China)

**Abstract:** In recent years, the Tanshan-Shangfu Nb-Ta-Li-Be metallogenic prospective area has been predicted in the southern of Jiuling area, northwest Jiangxi Province. Mineralization types include granite-type and aplite-type. Study on the formation age and genetic mechanism of rare metal deposits, is the key points of the enrichment and

收稿日期: 2023-08-05; 接受日期: 2023-12-12; 编辑: 尹淑萍

基金项目: 国家自然科学基金项目(42062006, 42273028); 核资源与环境国家重点实验室开放基金(2020NRE08); 中国核工业地质局地勘项目(202231, 202028-2)

作者简介: 党飞鹏(1986- ), 男, 高级工程师, 主要从事铀矿地质找矿勘查与研究, E-mail: feipengdang@163.com; 通讯作者: 张勇(1983- ), 男, 副教授, 主要从事铀矿地质教学与科研工作, E-mail: zhyey2004@163.com。

mineralization of rare metals in Jiuling area. Based on the study of the columbite-group minerals U-Pb geochronology, petrography and petrogeochemistry, to determine the diagenetic age and mineralization age, rock formation and magma source characters of the Nb-Ta-bearing aplite, and make analysis on its metallogenetic potential. The LA-ICP-MS niobite-tantalite U-Pb dating yields an age of  $142 \pm 1$  Ma, suggesting that the Nb-Ta-bearing aplite was formed in the Early Yanshanian period. The aplite is characterized by rich silica, alkali and aluminum, poor titanium and  $\Sigma$  REE, the wide range of Rb/Sr, and there exists obvious enrichment of niobium-tantalum-lithium-rubidium, and  $\text{CaO}/(\text{K}_2\text{O}+\text{Na}_2\text{O}) \leq 0.10$ ,  $\text{Al}_2\text{O}_3/\text{TiO}_2 > 160$ , high differentiation index. The REE diagram shows rightward incline and obvious negative Eu abnormality. The spider diagram of trace elements shows left side is uplifted and right side is gentle. All of these indicate that the aplite show features of highly differentiated S-type granitoids. It may be that the metamorphic argillaceous rocks of the Neoproterozoic Shuangqiaoshan Group in the Jiuling area were partially melted to form granitic magma, which during the transition stage from syn-collision to post-collision, and then to form highly fractionated aplite. In the late stage of magmatic differentiation and evolution, the interaction between fluid and melt leads to the enrichment of metal ore-forming elements like Nb-Ta-Li in the highly fractionated aplite. The Dongcao Nb-Ta-bearing aplite and the Nanling Nb-Ta-bearing granite, the Dahutang Nb-Ta-bearing granite porphyry have similar geochemical characteristics. Which is regarded as the main metallogenetic geological body in the Tanshan-Shangfu Nb-Ta-Li-Be metallogenetic prospective area.

**Key words:** niobium-tantalum deposit; aplite; geochemistry; niobite-tantalite U-Pb age; Jiuling area

**Fund support:** National Natural Science Foundation of China (42062006, 42273028); Open Fund of State Key Laboratory of Nuclear Resources and Environment (2020NRE08); China Nuclear Geology Co-funded by the Exploration Project (202231, 202028-2)

九岭-鄣公山钨锡多金属成矿带是在扬子板块东南缘中-新元古代裂谷及造山作用的基础上,经历早古生代褶皱隆升、晚古生代局部裂陷以及中生代强烈挤压隆升形成的构造-岩浆-成矿带(杨明桂等, 2004; 张勇, 2018)。九岭地区位于该成矿带的西段,是江西省重要的W-Sn-Cu-Mo-Li-Nb-Ta-U矿集区。九岭地区燕山期构造演化具有多阶段多幕次脉动式活动的特点,其动力学背景从碰撞阶段的挤压-伸展转变为后碰撞阶段的拉张(毛景文等, 2011; 丰成友等, 2012; 黄兰椿等, 2012, 2013; 项新葵等, 2015; 褚平利等, 2019; 赵正等, 2022)。燕山早期江南造山带再次活化,近EW向挤压应力作用造就了九岭地区NE向-NNE向褶皱构造和断裂构造体系,在南部形成多条NE向断裂构造,如兰溪-甘坊断裂、兰溪-上富断裂等。过渡阶段(145~130 Ma)构造应力场由挤压转换为拉张利于幔源物质上涌,进而诱发九岭地区壳源物质发生重熔形成过铝质酸性岩浆,沿NE向-NNE向断裂构造体系上侵,并经历了高程度分异结晶作用,促使Nb、Ta、Li等稀有金属矿化岩体的形成(李仁泽等, 2020)。

近些年在九岭地区南部新预测了潭山-上富Nb-Ta-Li-Be成矿远景区,发现了一批锂矿床和铌钽

矿床,成矿类型包括花岗岩型和细晶岩型两类。花岗岩型锂矿床已发现大港、白市化山、白石里、狮子岭、白水洞、金港等矿床(吴学敏等, 2016; 秦程, 2018; 王成辉等, 2019; 李仁泽等, 2020; 汪炎炎等, 2020; 曾晓建等, 2022; 刘泽等, 2023; Xu et al., 2023),含矿岩石为燕山早期第二阶段中细粒钠长石化白云母化花岗岩。细晶岩型铌钽矿床已发现党田、茜坑、东槽等矿床(吴学敏等, 2016; 谢军军等, 2018; 曾晓建等, 2022),含矿岩石包括燕山期细晶岩、霏细斑岩、伟晶岩等,多呈岩脉状。

伟晶岩(-细晶岩)成岩年龄的精确测定是探讨该类脉岩形成时构造环境和构造-岩浆作用过程的前提。伟晶岩(-细晶岩)和高分异花岗岩中锆石常常出现蜕晶质化,影响U-Pb同位素体系封闭,造成锆石结晶年龄失真(钟龙等, 2011; Che et al., 2015),但这些岩石中还有锡石、独居石、铌钽铁矿、磷灰石等含U副矿物。其中铌钽铁矿U-Pb同位素体系受蜕晶质化作用影响较小(Che et al., 2015, 2019),并且普通Pb含量极低,可作为U-Pb同位素定年矿物(钟龙等, 2011)。目前,该测年方法已在多个地区花岗岩、伟晶岩中成功应用(王锦荣等, 2020; 李杭等, 2020; 王核等, 2022; 李五福等,

2022; 吕书俊等, 2023; 刘新星等, 2023)。

对含铌钽岩脉、岩枝形成时代、成因类型、源岩属性及产出背景等问题的研究,有助于构建九岭地区燕山期构造-岩浆活动过程,有益于探讨该区铌钽等稀有金属成矿作用机制。本文在野外地质调查的基础上,对九岭地区南部东槽矿床含铌钽细晶岩开展了岩相学观察、LA-ICP-MS铌钽铁矿U-Pb定年和全岩地球化学分析,确定其成岩成矿时代并厘清了岩石类型和源区属性,与典型的含铌钽花岗岩进行类比,浅析其成矿潜力,以期为九岭地区燕山期稀有金属成矿机制研究和资源规模扩大提供基础数据支撑。

## 1 区域地质背景

九岭地区位于扬子板块东南缘江南造山带中段(图1a),基底为新元古界双桥山群浅变质岩,盖层为南华纪、震旦纪-中三叠世海相沉积地层和白垩纪-古近纪陆相地层(王迪, 2017; 段政等, 2019)。双桥山群( $Pt_3^1$ )广泛出露于九岭地区北部、西部和南部(图1b),是断陷环境下形成的海相泥砂质碎屑岩-火山碎屑岩-喷发熔岩组合的沉积建造(项新葵等, 2015; 蒋少涌等, 2015)。南华系( $Nh_1$ )-奥陶系(O)分布于北部(图1b),为一套连续的碳酸盐岩-

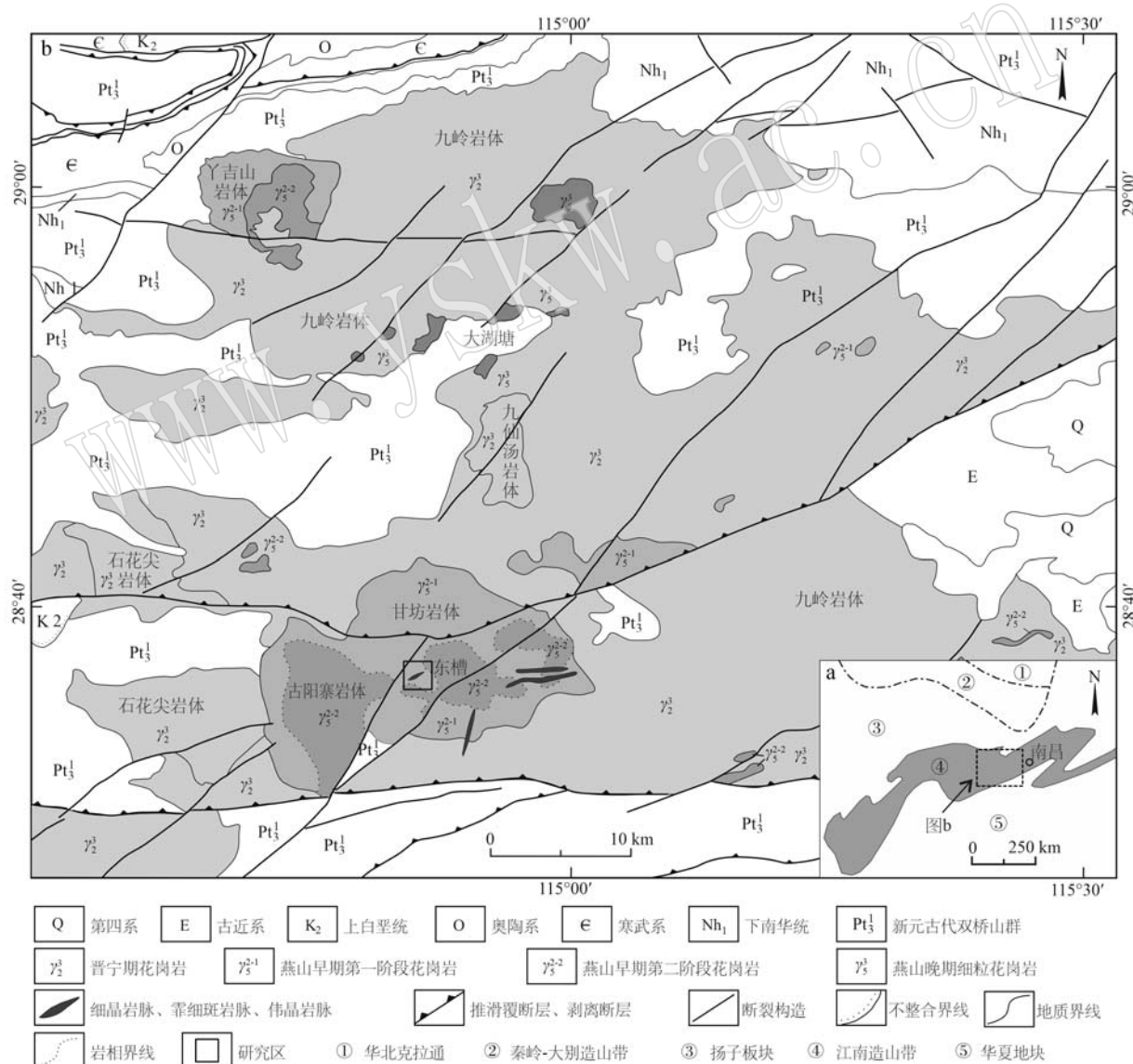


图1 九岭地区大地构造位置(a, 据张勇, 2018)及地质简图(b, 据段政等, 2019)

Fig. 1 Geotectonic location map (a, after Zhang Yong, 2018) and geological map of Jiuling area (b, after Duan Zheng et al., 2019)

硅质岩沉积组合。上三叠统( $T_3$ )为海陆交互相的含煤建造,下中侏罗统( $J_{1-2}$ )为河湖相沉积,上白垩统( $K_2$ )-新近纪(N)为红色砂岩、砂砾岩,分布在西部和南部(图1b)。基底双桥山群大都发生了褶皱作用,形成近EW向复式紧密线型褶皱。断裂构造以近EW向压扭性断裂和NE-NNE向走滑断裂为主,次为NW向、近SN向硅化断裂。侵入岩以晋宁期九岭岩体为主,次为晋宁期石花尖岩体、九仙汤岩体以及燕山期甘坊-古阳寨酸性侵入岩套、丫吉山岩体、大湖塘岩体等。晋宁期侵入岩大都侵位于双桥山群浅变质岩中,整体呈近EW向展布(图1b),出露面积大于4000 km<sup>2</sup>,是华南最大的花岗质岩基之一,也是钨多金属矿化的赋矿围岩。燕山期侵入岩多侵位于九岭岩体或中-新元古代浅变质岩系中,规模大小不一,具有多阶段脉动式侵入特征,岩石类型由早到晚主要有斑状黑(二)云母花岗岩、细粒黑云母花岗岩、白云母花岗岩、细粒花岗岩、花岗斑岩(脉)、细晶岩(脉)、霏细斑岩(脉)、伟晶岩(脉)等,与北部钨-锡-铜矿化及南部铌-钽-锂(-铀)等稀有金属成矿作用关系密切(蒋少涌等,2015;张勇等,2017,2020;张勇,2018)。

燕山期岩脉多发育在深成岩体的顶部,大都沿断裂构造充填,往往产出铌钽等稀有金属矿化。依据金属矿物组合和地球化学特征的不同,含矿岩脉分为锂铯钽型(LCT型)和铌钇氟型(NYF型)两类,前者地球化学特征相似于过铝质S型花岗岩,后者相似于A型花岗岩(张辉等,2021)。稀有金属矿化多与高分异花岗岩密切相关,铌钽等矿化大都产在浅成的酸性富碱岩脉、岩枝中(刘莹等,2018),如伟晶岩脉、细晶岩脉等。

## 2 矿床地质特征

东槽铌钽矿床位于九岭南段燕山期甘坊岩体的中部(图1b)。矿床内出露燕山早期第一阶段中粗粒斑状黑云母花岗岩和燕山晚期细粒(白云母)花岗岩、花岗斑岩(脉)、细晶岩(脉)、霏细斑岩(脉)、伟晶岩(脉)等。断裂构造以近SN向、NE向断裂为主。近SN向断裂大多为硅化破碎带,倾向东,倾角65°~88°,带内发育灰色-红褐色硅质-玉髓脉、硅化角砾岩、硅化碎裂岩等,常见黄铁矿化、硅化、赤铁矿化和紫黑色萤石化,是铀矿化的含矿构造。NE向断裂以硅化断裂为主,倾向北西,倾角56°~84°,带内

充填硅化角砾岩、硅化碎裂岩,在研究区大都被细晶岩脉、花岗斑岩脉充填(图2),可见钠长石化、云英岩化、白云母化、紫色萤石化等,往往产出铌钽矿化。

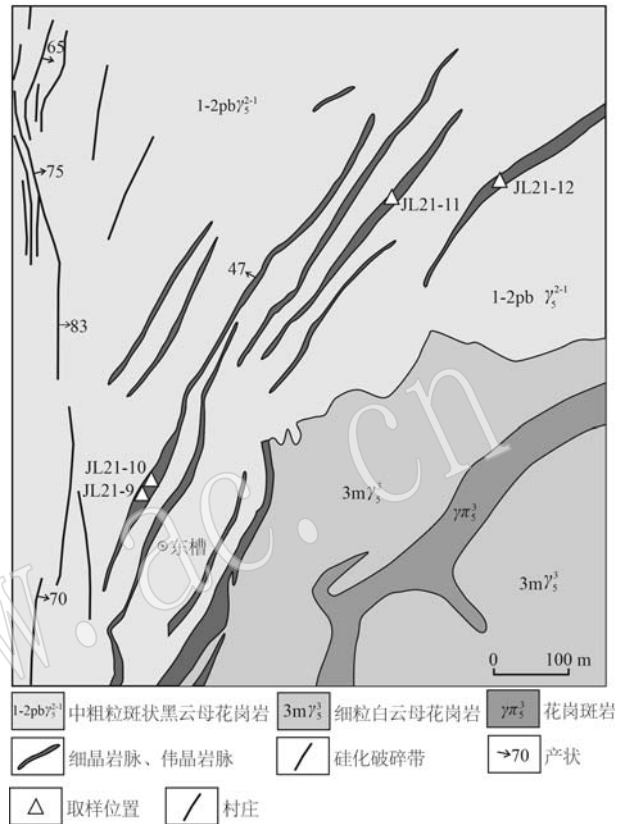


图2 东槽矿床地质简图  
Fig. 2 Geological map of Dongcao deposit

细晶岩(脉)沿NE向断裂呈岩脉状发育,单条走向长200~1500 m,出露宽5~8 m,最宽达40 m,走向50°~60°,倾向NW,倾角40°~70°,多呈近平行带组状展布(图2)。已发现3条规模较大的含铌钽细晶岩脉,岩石类型以蚀变斜长细晶岩为主,矿石矿物有铌钽铁矿、铌铁矿、钽铁矿、细晶石以及锂云母等。矿化段细晶岩脉中氧化铌含量为0.010%~0.019%,氧化钽含量为0.015%~0.026%,氧化锂含量为0.100%~0.800%,以铌钽矿化为主,最高品位为0.040%,发育钠长石化、白云母化、黄玉化、云英岩化等热液蚀变。野外调查发现,在细晶岩脉膨大部位,氧化铌和氧化钽含量增高,厚度变大。

含铌钽细晶岩野外露头呈白色-灰白色(图3a),以(变余)细粒花岗结构为主,块状构造,矿物组成为斜长石(35%±)、钾长石(23%±)、石英(25%±)、白云母(16%±)(图3b)。斜长石为灰白色,半自形板状,粒径0.2~0.5 mm,发育高岭土化(图3c);钾

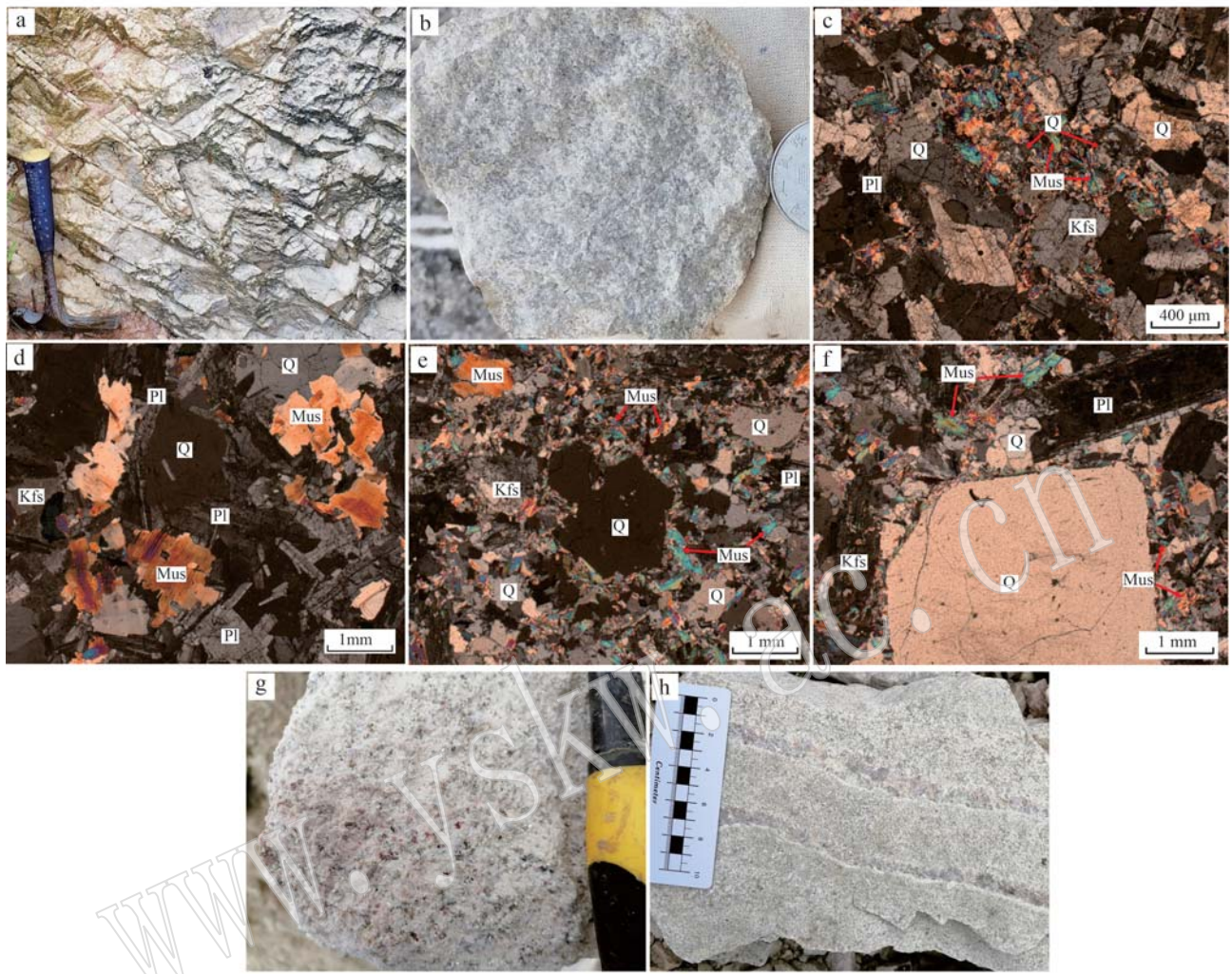


图3 东槽含铌钽细晶岩野外及显微照片(正交偏光)

Fig. 3 Specimen and microscopic photos of the Nb-Ta-bearing aplite in Dongcao deposit (cross-polarized light)

a—含铌钽细晶岩野外露头,灰白色,整体呈北东向脉状侵入中粗粒斑状黑云母花岗岩; b—细晶岩手标本,新鲜,细粒花岗结构,可见片状(锂)白云母; c—钾长石(Kfs)、斜长石(Pl)边缘蚀变为白云母(Mus); d—原生(锂)白云母,片径0.35~1.20 mm; e—云英岩化,绢云母、白云母(Mus)交代钾长石(Kfs)、斜长石(Pl); f—云英岩化,绢云母、白云母(Mus)交代钾长石(Kfs)、斜长石(Pl); g—含铌钽细晶岩手标本,见玫瑰色云母; h—细晶岩及晚期充填的长石石英脉

a—field outcrop of Nb-Ta-bearing aplite, grayish-white, it is vein which is produced in medium-coarse porphyritic biotite granite; b—hand specimens of aplite, fresh, fine grained texture, inclusions muscovite; c—the edge of feldspar is altered into muscovite; d—inclusions primary muscovite with a diameter of 0.35~1.20 mm; e—greisenization, sericite and muscovite metasomatic feldspar; f—greisenization, sericite and muscovite metasomatic feldspar; g—hand specimens of Nb-Ta-bearing aplite, inclusions rose-coloured muscovite; h—aplite and late-period quartz-feldspar vein

长石呈板状,粒径0.25~0.55 mm;石英呈他形粒状,粒径约0.5 mm;(锂)白云母呈鳞片状,片径0.35~1.20 mm(图3d)。含铌钽细晶岩中矿石矿物有铌钽铁矿、铌铁矿、钽铁矿和少量细晶石,以及锂云母、锂白云母,发育钠长石化、白云母化、绢云母化、云英岩化等热液蚀变,可见绢云母、白云母交代长石等现象(图3e,3f)。矿化段细晶岩脉蚀变程度增强,可见玫瑰色云母(图3g);局部可见伟晶岩化,长石粗晶、石

英粗晶(图3h),偶见二云母花岗岩岩屑。

### 3 样品与测试

#### 3.1 样品

研究样品采自东槽铌钽矿床内NE向细晶岩脉,采样位置详见图2。U-Pb同位素LA-ICP-MS测定所用铌钽铁矿选自样品JL21-9,岩相学观察和全岩主量

元素、微量元素和稀土元素含量检测选用新鲜岩石样品 JL21-10、JL21-11、JL21-12, 岩石类型均为斜长细晶岩。

### 3.2 全岩主量、微量元素及稀土元素分析

主量元素检测采用四硼酸锂-偏硼酸锂混合熔剂,与样品混匀后在1150~1250℃下熔融并铸成玻璃熔片,借助岛津X荧光光谱仪进行测定。X光管最大电压40 kV,最大电流95 mA,利用康普顿射线为内标校正基体效应。各元素含量测量范围介于0.002%~99%之间。微量元素及稀土元素采用电感耦合等离子体质谱法测定,样品前处理方式为封闭溶矿,用氢氟酸、高氯酸、硝酸、盐酸等处理,检测仪器为美国PerkinElmer公司NexION2000B型电感耦合等离子体质谱仪,选择不同质核比的离子检测某个离子的强度,计算某种元素的含量。仪器主要性能[Li(7)≤3% RSD, Y(89)≤3% RSD, Ti(204)≤3% RSD],雾化气流量0.98 L/min,等离子体气流1.2 L/min,射频功率1200 W,用内标法进行校正。上述项目测定均在核工业二七〇研究所分析测试中心完成,测定结果质量监控精密度、准确度等均满足DZ/T0130中相关项目质量要求。

### 3.3 铌钽铁矿U-Pb年龄分析

铌钽铁矿U-Pb定年在中国地质调查局铀矿地质重点实验室完成。通过联用Applied Spectra

Reslution LR 193nm ArF准分子激光剥蚀系统与Agilent7900四极杆ICP-MS仪器进行测试,激光束斑直径为43 μm,激光能量密度为3 mJ/cm<sup>2</sup>,频率为6 Hz,采用Coltan139作为外标。元素含量采用美国国家标样技术研究院的人工合成硅酸盐标准参考物质NISTSRM610作为外标(Pearce *et al.*, 1997; Gao *et al.*, 2002),<sup>29</sup>Si作为内标校正。详细的测试流程和参数设置可参考文献(Che *et al.*, 2015)。数据处理使用软件ICPMSDataCal 10.1(Liu *et al.*, 2010),铌钽铁矿的谐和年龄图绘制和加权平均年龄计算使用软件Isoplot3.0(Ludwing, 2003)。

## 4 分析结果

### 4.1 铌钽铁矿U-Pb年龄

含铌钽细晶岩样品(JL21-9)中铌钽铁矿呈黄褐色,为半自形-自形板柱状,大小为(110~145) μm×(80~105) μm。铌钽铁矿BSE图像较暗,为均一不分带结构,无包裹体、无裂隙(图4a)。LA-ICP-MS U-Pb同位素测定结果详见表1, Th含量为0.38×10<sup>-6</sup>~85.0×10<sup>-6</sup>(平均值为4.36×10<sup>-6</sup>), U含量为95×10<sup>-6</sup>~3420×10<sup>-6</sup>(平均值为462×10<sup>-6</sup>), Th/U值0.002~0.025。

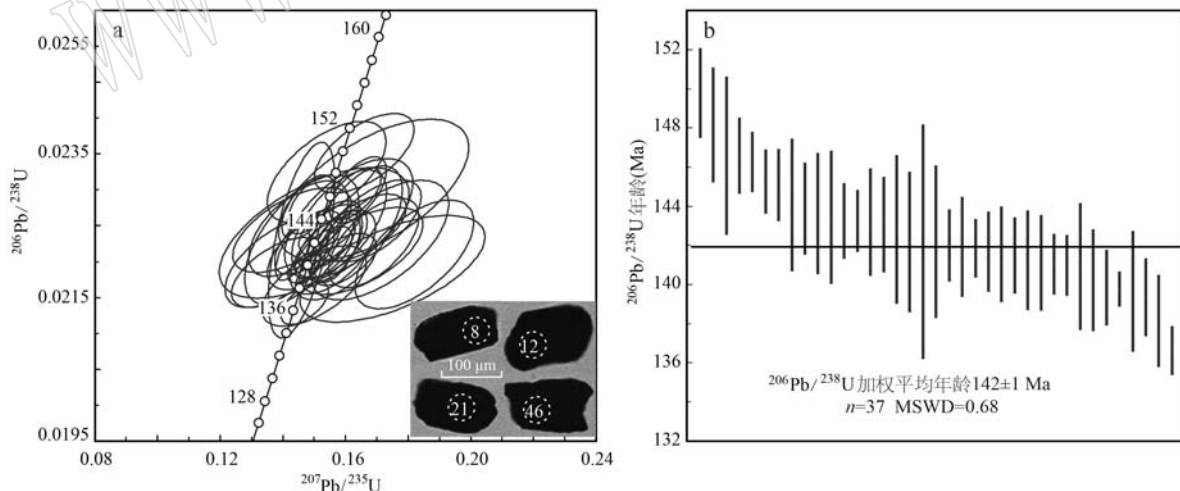


图4 东槽含铌钽细晶岩铌钽铁矿U-Pb谐和图(a)和加权平均<sup>206</sup>Pb/<sup>238</sup>U年龄图(b)

Fig. 4 Concordia diagrams of the Niobite-tantalite U-Pb dating (a) and weighted mean diagrams of <sup>206</sup>Pb/<sup>238</sup>U apparent ages (b) for the Nb-Ta-bearing aplite in Dongcao deposit

对48颗铌钽铁矿进行U-Pb同位素年龄测定,获得37个有效点,<sup>206</sup>Pb/<sup>238</sup>U年龄值均分布于谐和曲线上(图4a)。加权平均年龄为142±1 Ma(MSWD=0.68)(图4b),是铌钽铁矿的结晶年龄,表明含铌

钽细晶岩的成岩、成矿时代均在燕山早期(早白垩世)。

### 4.2 主量元素特征

如表2所示,东槽含铌钽细晶岩富硅(SiO<sub>2</sub>)含量

表 1 东槽含铌钽细晶岩 LA-ICP-MS 钨钽铁矿 U-Th-Pb 分析结果  
Table 1 LA-ICP-MS niobite-tantalite U-Th-Pb dating data of the Nb-Ta-bearing aplite in Dongcao deposit

分析点号	$w_B / 10^{-6}$						同位素比值						同位素年龄/Ma		
	Pb	Th	U	$^{207}\text{Pb}/^{206}\text{Pb}$	$1\sigma$	$^{207}\text{Pb}/^{235}\text{U}$	$1\sigma$	$^{206}\text{Pb}/^{238}\text{U}$	$1\sigma$	$^{207}\text{Pb}/^{206}\text{Pb}$	$1\sigma$	$^{207}\text{Pb}/^{235}\text{U}$	$1\sigma$	$^{206}\text{Pb}/^{238}\text{U}$	$1\sigma$
m21-5-01	6.60	5.01	957	0.051 4	0.001 6	0.157 4	0.004 8	0.022 2	0.000 3	261	65	148	4	141	2
m21-5-04	2.60	1.83	580	0.051 1	0.003 1	0.156 0	0.009 0	0.022 1	0.000 4	247	115	147	8	141	2
m21-5-05	1.90	2.59	367	0.052 5	0.003 8	0.163 0	0.010 0	0.022 5	0.000 6	309	165	153	9	143	3
m21-5-07	0.39	0.92	197	0.054 3	0.003 3	0.169 0	0.010 0	0.022 6	0.000 4	384	115	159	9	144	2
m21-5-08	1.45	0.96	159	0.051 9	0.003 2	0.157 0	0.008 5	0.021 9	0.000 3	282	105	148	8	140	2
m21-5-09	2.50	4.51	1124	0.051 5	0.001 8	0.163 0	0.005 5	0.023 0	0.000 2	264	70	153	5	146	2
m21-5-10	1.90	2.23	330	0.048 0	0.004 6	0.154 0	0.012 5	0.023 3	0.000 5	101	165	145	12	148	3
m21-5-11	0.03	0.42	122	0.045 8	0.004 0	0.139 0	0.011 5	0.022 0	0.000 4	-11	145	132	10	140	3
m21-5-12	0.57	0.54	99	0.049 3	0.003 8	0.151 0	0.010 5	0.022 2	0.000 4	164	120	143	9	142	2
m21-5-13	1.40	0.98	208	0.053 3	0.007 0	0.169 0	0.020 0	0.023 0	0.000 7	341	235	159	20	147	4
m21-5-15	3.37	3.82	594	0.051 2	0.001 8	0.157 0	0.005 5	0.022 2	0.000 3	252	70	148	5	142	2
m21-5-16	9.70	2.64	284	0.053 3	0.003 2	0.165 0	0.009 5	0.022 5	0.000 3	340	115	155	9	143	2
m21-5-17	2.38	0.64	130	0.046 8	0.003 7	0.145 0	0.010 5	0.022 5	0.000 4	40	130	137	9	143	3
m21-5-18	0.95	0.44	278	0.051 7	0.004 2	0.161 0	0.013 5	0.022 6	0.000 6	271	160	152	13	144	3
m21-5-19	1.40	1.35	534	0.051 2	0.003 4	0.166 0	0.010 5	0.023 5	0.000 4	250	125	156	9	150	2
m21-5-20	2.40	3.88	522	0.050 9	0.003 2	0.158 0	0.010 0	0.022 5	0.000 5	235	125	149	9	144	3
m21-5-21	23.0	85.0	3420	0.047 5	0.001 3	0.146 0	0.007 0	0.022 3	0.000 9	74	55	138	6	142	6
m21-5-22	0.07	0.59	112	0.050 2	0.004 1	0.150 0	0.011 0	0.021 7	0.000 4	205	140	142	10	138	2
m21-5-25	4.00	3.59	850	0.051 7	0.001 9	0.164 0	0.006 0	0.023 0	0.000 3	273	80	154	5	147	2
m21-5-26	1.08	4.06	628	0.047 4	0.001 7	0.149 0	0.005 0	0.022 8	0.000 3	70	70	141	5	145	2
m21-5-27	16.1	3.96	262	0.059 7	0.004 7	0.182 0	0.012 5	0.022 1	0.000 5	594	155	170	12	141	3
m21-5-28	1.32	0.51	100	0.054 0	0.004 4	0.165 0	0.013 0	0.022 2	0.000 4	372	140	155	11	141	3
m21-5-29	1.29	2.33	661	0.046 9	0.001 2	0.143 1	0.003 6	0.022 1	0.000 2	46	48	136	3	141	2
m21-5-30	0.85	1.73	440	0.055 6	0.005 5	0.171 0	0.014 5	0.022 3	0.000 6	437	180	160	13	142	4
m21-5-31	0.77	0.40	135	0.046 2	0.003 8	0.143 0	0.012 5	0.022 4	0.000 4	9	140	136	11	143	2
m21-5-32	0.38	0.38	95	0.048 6	0.007 5	0.150 0	0.020 0	0.022 4	0.000 6	127	230	142	17	143	4
m21-5-33	0.84	0.93	174	0.058 0	0.007 0	0.175 0	0.019 5	0.021 9	0.000 5	528	245	164	18	140	3
m21-5-34	3.20	3.17	519	0.050 0	0.002 1	0.155 0	0.006 5	0.022 5	0.000 3	196	85	146	6	143	2
m21-5-36	0.95	2.90	432	0.048 2	0.002 3	0.148 0	0.007 0	0.022 3	0.000 3	109	90	140	7	142	2
m21-5-37	2.30	1.40	364	0.047 2	0.001 9	0.148 0	0.005 5	0.022 8	0.000 3	57	75	140	5	145	2
m21-5-38	1.61	2.54	287	0.050 2	0.001 9	0.153 0	0.006 0	0.022 1	0.000 2	203	75	145	5	141	2
m21-5-39	0.97	0.59	150	0.045 8	0.003 1	0.138 0	0.009 5	0.021 9	0.000 3	-13	120	131	9	139	2
m21-5-40	1.90	1.82	423	0.047 5	0.003 6	0.146 0	0.012 0	0.022 3	0.000 6	74	145	138	11	142	4
m21-5-42	1.25	1.20	222	0.050 2	0.002 2	0.154 0	0.006 0	0.022 3	0.000 2	204	75	145	5	142	2
m21-5-46	3.30	4.25	370	0.055 1	0.003 4	0.169 0	0.009 5	0.022 3	0.000 4	415	115	159	9	142	3
m21-5-47	1.65	1.74	275	0.049 8	0.001 8	0.147 0	0.005 0	0.021 4	0.000 2	184	70	139	5	137	1
m21-5-48	7.10	5.52	713	0.048 6	0.001 1	0.146 9	0.003 5	0.021 9	0.000 1	129	47	139	3	140	1

表2 东槽含铌钽细晶岩和大湖塘含铌钽花岗斑岩主量元素( $w_{\text{B}}/\%$ )、微量元素和稀土元素( $w_{\text{B}}/10^{-6}$ )分析结果

Table 2 Major elements( $w_{\text{B}}/\%$ ), rare elements and rare earth elements( $w_{\text{B}}/10^{-6}$ ) analysis results of the Nb-Ta-bearing aplite in Dongcao deposit and the Nb-Ta-bearing granite-porphyry in Dahutang district

岩石类型 样品	斜长细晶岩(东槽)			花岗斑岩(大湖塘)		
	JL21-10	JL21-11	JL21-12	PM04	H6334	H6336
SiO <sub>2</sub>	71.5	70.7	71.6	71.5	72.8	73.8
TiO <sub>2</sub>	0.09	0.10	0.07	0.02	0.03	0.04
Al <sub>2</sub> O <sub>3</sub>	16.2	16.5	16.8	16.1	16.7	16.2
<sup>T</sup> Fe <sub>2</sub> O <sub>3</sub>	1.38	1.41	0.73	0.45	0.97	0.80
Fe <sub>2</sub> O <sub>3</sub>	0.24	0.31	0.24	0.23	0.15	0.12
FeO	1.16	1.13	0.51	0.24	0.84	0.69
MnO	0.12	0.22	0.17	0.07	0.09	0.04
MgO	0.05	0.05	0.05	0.01	0.01	0.01
CaO	0.57	0.63	0.69	0.37	0.03	0.04
Na <sub>2</sub> O	4.53	4.86	4.81	5.73	2.60	3.69
K <sub>2</sub> O	3.32	2.36	2.32	3.48	4.25	3.83
P <sub>2</sub> O <sub>5</sub>	0.59	0.54	0.58	0.40	0.49	0.36
LOI	0.77	1.86	2.01	1.18	/	/
总量	100.51	100.71	100.49	99.77	/	/
K <sub>2</sub> O+Na <sub>2</sub> O	7.85	7.22	7.13	9.21	6.85	7.52
CaO/(K <sub>2</sub> O+Na <sub>2</sub> O)	0.073	0.087	0.097	0.041	0.004	0.005
Al <sub>2</sub> O <sub>3</sub> /TiO <sub>2</sub>	180	165	239	1 073	557	405
A.R.	2.76	2.45	2.38	3.54	2.38	2.72
DI	90.9	89.8	90.6	95.5	89.6	92.1
A/CNK	1.34	1.41	1.44	1.16	1.87	1.58
ANK	1.47	1.57	1.61	1.22	1.88	1.59
C/FM	1.03	1.12	2.13	2.19	0.08	0.14
A/FM	16.1	16.1	28.4	51.8	25.8	30.3
Rb	1 440	1 210	1 190	1 342	1 000	758
Sr	8.7	41.7	48.3	22	2.77	5.69
Y	1.62	1.5	2.01	2.3	2.9	3.28
Zr	14.5	8.1	8.7	29	72.8	51.1
Hf	0.938	1.1	1.02	2.4	6.3	4.1
Nb	87.9	89.4	99.8	54	34.3	32.6
Ta	157	183	157	32	23.8	21.1
Ba	9.54	11.7	8.69	1.5	1.68	2.64
Th	0.764	0.985	0.758	2.3	4.27	3.6
U	11.7	3.08	2.23	13	6.83	5.63
Pb	2.58	1.48	1.01	5.8	6.34	5.63
Ti	514	593	433	149	180	240
P	2 568	2 372	2 529	1 744	2 137	1 570
Li	1 923	2 450	2 630	375	123	954
Be	58.8	79.2	86.7	5.2	-	-
Sn	64.0	78.4	67.9	66	-	-
Rb/Sr	166	29.0	24.6	61.0	361	133
Zr/Hf	15.5	7.36	8.53	12.1	11.6	12.5
Nb/Ta	0.56	0.49	0.64	1.69	1.44	1.55
Ba+Sr	18.2	53.4	57.0	23.5	4.45	8.33
Th/U	0.07	0.32	0.34	0.18	0.63	0.64
La	0.75	0.56	0.64	1.10	3.31	3.18
Ce	1.47	1.23	1.44	3.10	7.90	7.50
Pr	0.14	0.12	0.14	0.29	0.93	0.87
Nd	0.49	0.44	0.52	1.03	3.25	3.06
Sm	0.22	0.18	0.18	0.34	0.96	0.84
Eu	0.01	0.02	0.01	0.01	0.02	0.02
Gd	0.25	0.21	0.20	0.29	0.78	0.84
Tb	0.06	0.05	0.05	0.06	0.13	0.13
Dy	0.34	0.28	0.26	0.38	0.71	0.77
Ho	0.05	0.05	0.04	0.06	0.10	0.11
Er	0.10	0.14	0.12	0.17	0.30	0.33
Tm	0.02	0.02	0.02	0.03	0.06	0.06
Yb	0.09	0.14	0.12	0.21	0.45	0.43
Lu	0.01	0.02	0.01	0.03	0.07	0.05
ΣREE	4.00	3.44	3.74	7.10	19.0	18.2
LREE/HREE	3.37	2.82	3.60	4.77	6.30	5.69
δEu	0.10	0.29	0.21	0.09	0.07	0.07
(La/Yb) <sub>N</sub>	5.74	2.95	3.98	3.76	5.28	5.30
(La/Sm) <sub>N</sub>	2.17	2.08	2.36	2.09	2.23	2.44
(Gd/Yb) <sub>N</sub>	2.18	1.28	1.45	1.14	1.43	1.62
Zr+Nb+Ce+Y	105	100	112	88	118	94.5

为70.7%~71.6%),富钠贫钾( $\text{Na}_2\text{O}/\text{K}_2\text{O}=1.78\sim2.16$ ),富碱( $\text{K}_2\text{O}+\text{Na}_2\text{O}=7.13\%\sim7.85\%$ ),在 $\text{SiO}_2-(\text{K}_2\text{O}+\text{Na}_2\text{O})$ 图上落点于花岗岩区(图5a),属钙碱性-碱性系列花岗岩(图5b、5c);并具较低的 $\text{CaO}$ 含量(0.57%~0.69%)和 $\text{CaO}/(\text{K}_2\text{O}+\text{Na}_2\text{O})$ 比值(0.07~0.10);富铝( $\text{Al}_2\text{O}_3$ 含量为16.2%~

16.8%), $\text{A/CNK}=1.34\sim1.44>1.30$ ,属强过铝质岩石(图5d); $\text{TiO}_2$ 含量低(0.07%~0.10%),与副矿物中少见钛铁矿、磷灰石的现象一致; $\text{Al}_2\text{O}_3/\text{TiO}_2$ 值较高(165~239);富磷( $\text{P}_2\text{O}_5$ 含量0.54%~0.59%),贫铁镁( $\text{TFeO}$ 含量0.73%~1.41%、 $\text{MgO}$ 含量0.05%), $\text{Mg}^{\#}$ 值低(7.6~13.8,平均9.75)。

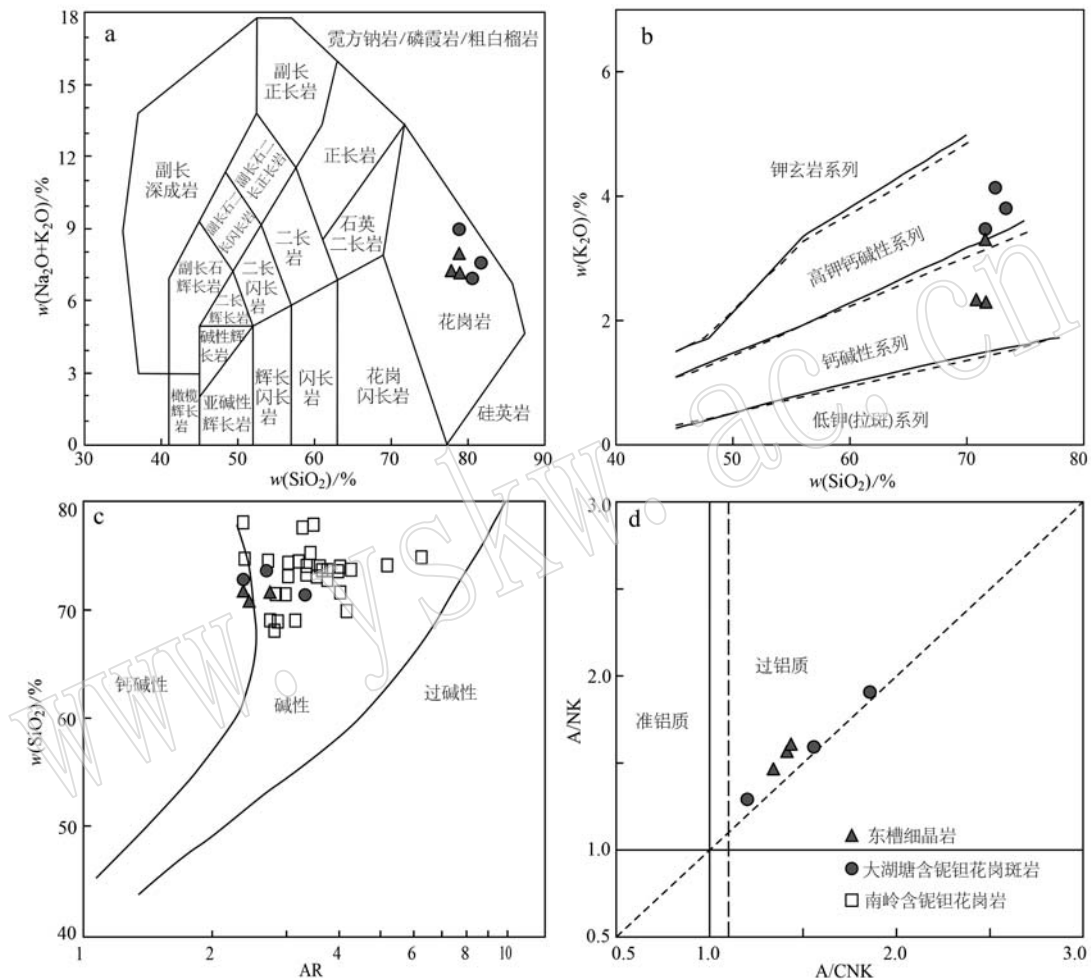


图5 主量元素图解

Fig. 5 Major element diagrams

a— $(\text{K}_2\text{O}+\text{Na}_2\text{O})-\text{SiO}_2$ 图(据Middlemost, 1994); b— $\text{K}_2\text{O}-\text{SiO}_2$ 图(据Peccerillo and Taylor, 1976); c— $\text{SiO}_2-\text{AR}$ 图(据Wright, 1969); d— $\text{A/NK}-\text{A/CNK}$ 图(据Maniar and Piccoli, 1989);南岭含铌钽花岗岩数据引自陈骏等(2008);大湖塘含铌钽花岗斑岩数据引自刘莹等(2018)和褚平利等(2019)

a— $(\text{K}_2\text{O}+\text{Na}_2\text{O})-\text{SiO}_2$  diagram (after Middlemost, 1994); b— $\text{K}_2\text{O}-\text{SiO}_2$  diagram (after Peccerillo and Taylor, 1976); c— $\text{SiO}_2-\text{AR}$  diagram (after Wright, 1969); d— $\text{A/NK}-\text{A/CNK}$  diagram (after Maniar and Piccoli, 1989); the datas of Nanling Nb-Ta-bearing granite are quoted from Chen Jun *et al.* (2008); the datas of Dahutang Nb-Ta-bearing granite-porphyry are quoted from Liu Ying *et al.* (2008) and Chu Pingli *et al.* (2019)

#### 4.3 微量及稀土元素特征

东槽含铌钽细晶岩富集大离子亲石元素Rb、U、Pb、P和高场强元素Ta,明显亏损大离子亲石元素Ba、Sr和高场强元素Nb、Ti、Rb含量为 $1.190\times10^{-6}\sim$

$1.440\times10^{-6}>1.100\times10^{-6}$ , $\text{Ba}+\text{Sr}=(18.2\sim57.0)\times10^{-6}<60\times10^{-6}$ ,微量元素原始地幔标准化蛛网图显示左侧隆起和右侧平缓的特征(图6a),具有较高的Li( $>1.900\times10^{-6}$ )、Nb( $>85\times10^{-6}$ )、Ta( $>155\times10^{-6}$ )

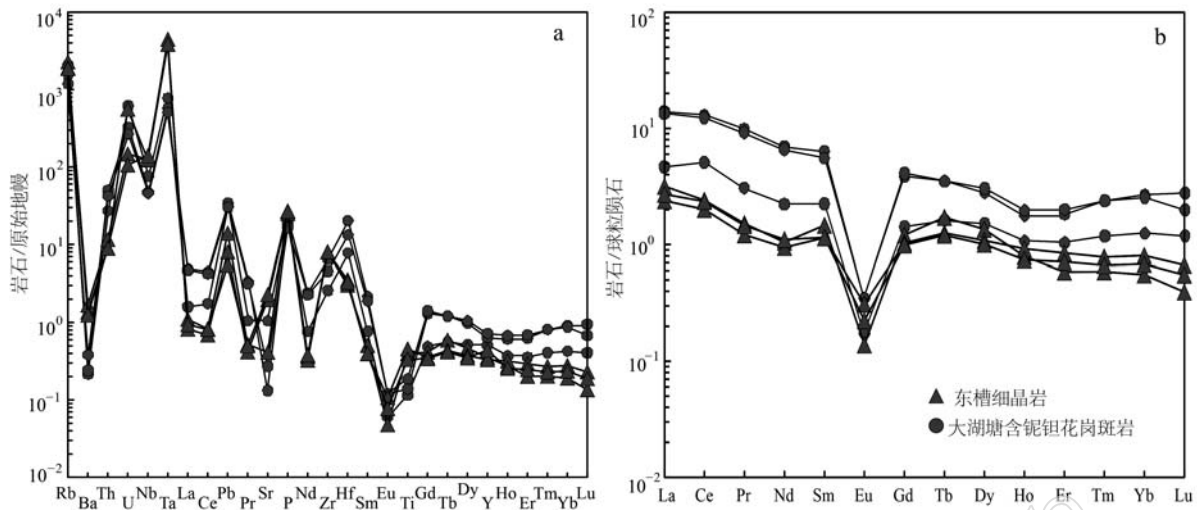


图 6 微量元素原始地幔标准化蛛网图(a)和稀土元素球粒陨石标准化配分曲线(b)[标准化数值引自 Sun and McDonough (1989)]

Fig. 6 Primitive mantle-normalized trace element spider diagram (a) and chondrite-normalized REE distribution pattern (b) [normalized values after Sun and McDonough (1989)]  
大湖塘含铌钽花岗斑岩数据引自刘莹等(2018)和褚平利等(2019)

the data of Dahutang Nb-Ta-bearing granite-porphyry are quoted from Liu Ying et al. (2018) and Chu Pingli et al. (2019)

和 Sn ( $> 64 \times 10^{-6}$ ) 含量(表 2)。稀土总量极低 ( $\Sigma\text{REE} = 3.44 \times 10^{-6} \sim 4.00 \times 10^{-6}$ )，可能与花岗质岩浆高程度结晶分异的晚期稀土元素进入流体相有关(彭花明等, 2014)。轻稀土元素相对富集且分馏弱,LREE/HREE 值  $2.82 \sim 3.60$ 、 $(\text{La}/\text{Sm})_N = 2.08 \sim 2.36$ ; Eu 强烈亏损,  $\delta\text{Eu} = 0.10 \sim 0.29$ 。稀土元素球粒陨石标准化配分曲线呈弱右倾的海鸥型(图 6b)。

## 5 讨论

### 5.1 含铌钽细晶岩成岩与成矿时代

九岭地区燕山期侵入岩岩石类型从早到晚依次为斑状黑(二)云母花岗岩→细粒黑云母花岗岩、白云母花岗岩→花岗斑岩→细粒花岗岩(脉)、细晶岩(脉)、霏细斑岩(脉)、伟晶岩(脉),构造-岩浆-成矿活动持续时间长,具多阶段脉动式活动的特点(刘莹等, 2018; 陈茂松等, 2020),主要集中在晚侏罗世-早白垩世( $152 \sim 128$  Ma)(丰成友等, 2012; 黄兰椿等, 2012, 2013; 项新葵等, 2015; 吴显愿等, 2019; 褚平利等, 2019; 陈茂松等, 2020; 赵正等, 2022)。

本文利用 LA-ICP-MS 铌钽铁矿 U-Pb 定年测得东槽含铌钽细晶岩成岩年龄为  $142 \pm 1$  Ma,与大湖塘含铌钽花岗斑岩铌钽铁矿 U-Pb 同位素年龄一致( $144 \pm 5$  Ma, 刘莹等, 2018),同属早白垩世成岩

成矿阶段,是九岭地区燕山期高分异花岗岩形成的主要时期,也是铌钽等稀有金属矿化的主成矿期。

### 5.2 含铌钽细晶岩成因类型与源区特征

#### 5.2.1 成因类型

I型花岗岩源于陆壳或者洋壳中基性岩石的部分熔融,S型花岗岩是中上地壳沉积岩类岩石部分熔融的产物。东槽含铌钽细晶岩稀土元素配分曲线呈弱右倾的海鸥型(图 6b),负 Eu 异常明显,与 I型花岗岩稀土元素配分曲线较小斜率且弱负铕异常(或无铕异常)的特征不相符;高场强元素 Zr、Nb、Ce 和 Y 含量都偏低, $Zr+Nb+Ce+Y = 100 \times 10^{-6} \sim 112 \times 10^{-6}$ ,低于 A型花岗岩的下限值( $350 \times 10^{-6}$ , Whalen et al., 1987),并在岩石类型判别图解上大都落入 S型花岗岩区(图 7a、7b)。

微量元素和稀土元素地球化学特征可指示花岗岩的演化程度(陈骏等, 2008),碱金属含量(Li、Rb、Cs 等)和 Rb/Sr 值变大,Zr/Hf、Nb/Ta 和 K/Rb 值降低,稀土元素总量降低,代表其岩浆演化程度越高(Linnen and Keppler, 2002)。富铝( $A/\text{CNK} > 1.30$ ),是典型的强过铝质花岗岩;高的分异指数( $DI \geq 90$ ),高的 Li( $> 1900 \times 10^{-6}$ )、Rb( $> 1100 \times 10^{-6}$ )、Cs( $> 270 \times 10^{-6}$ )含量,较低的 Zr/Hf 值( $7.36 \sim 15.5$ )和 Nb/Ta 值( $0.49 \sim 0.64$ )以及变化范围大的 Rb/Sr 值( $24.6 \sim 165$ ),岩石矿物组成中含有锂云母、锂白云母和铌钽

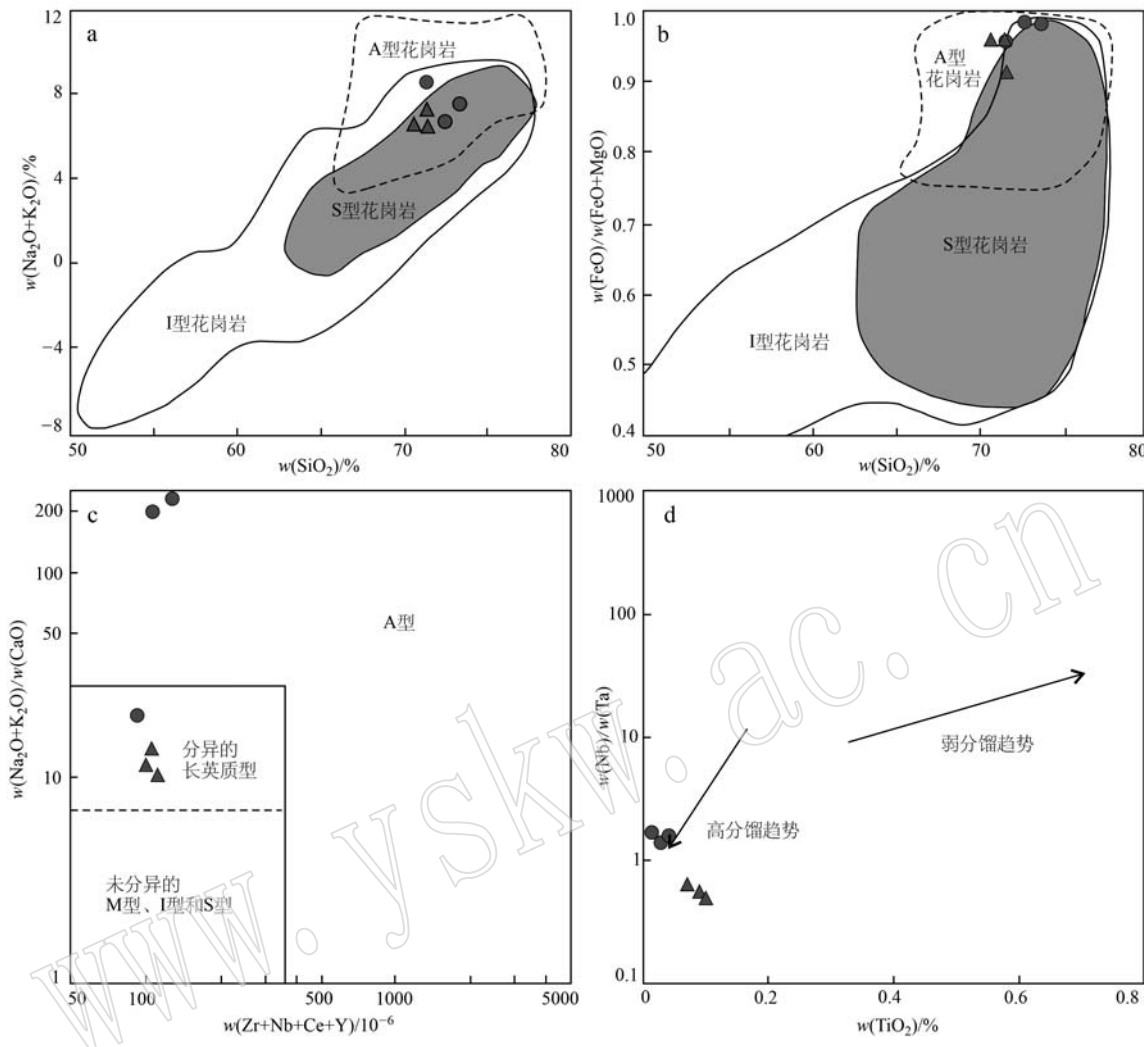


图 7 岩石类型判别图解

Fig. 7 Discrimination diagrams for the rock types

a— $(\text{Na}_2\text{O}+\text{K}_2\text{O})-\text{SiO}_2$  图(据 Frost *et al.*, 2001); b— $\text{FeO}/(\text{FeO}+\text{MgO})-\text{SiO}_2$  图(据 Frost *et al.*, 2001); c— $(\text{Na}_2\text{O}+\text{K}_2\text{O})/\text{CaO}- (\text{Zr}+\text{Nb}+\text{Ce}+\text{Y})$  图(据 Whalen *et al.*, 1987); d— $\text{Nb}/\text{Ta}-\text{TiO}_2$  图(据 Cao *et al.*, 2002); 图例同图 6

a— $(\text{Na}_2\text{O}+\text{K}_2\text{O})-\text{SiO}_2$  diagram (after Frost *et al.*, 2001); b— $\text{FeO}/(\text{FeO}+\text{MgO})-\text{SiO}_2$  diagram (after Frost *et al.*, 2001); c— $(\text{Na}_2\text{O}+\text{K}_2\text{O})/\text{CaO}- (\text{Zr}+\text{Nb}+\text{Ce}+\text{Y})$  diagram (after Whalen *et al.*, 1987); d— $\text{Nb}/\text{Ta}-\text{TiO}_2$  diagram (Cao *et al.*, 2002); same symbols as in Fig. 6

铁族矿物，并落点于分异的长英质型区（图 7c），表明该细晶岩是花岗质岩浆遭受高程度分异结晶的产物。在  $\text{TiO}_2-\text{Nb}/\text{Ta}$  关系图上也显示出高分馏趋势（图 7d）。极低的稀土总量 ( $\Sigma \text{REE} \leq 4.00 \times 10^{-6}$ )，稀土元素配分曲线呈弱右倾的海鸥型，以及 LREE/HREE 值、 $\delta \text{Eu}$  值与分异指数 DI 呈负相关关系，暗示岩浆演化过程存在明显的富 LREE 矿物（如独居石、褐帘石）和富 Eu 矿物（如斜长石）的分离结晶（项新葵等, 2015），表明该细晶岩属高分异花岗岩。

综上所述，东槽含铌钽细晶岩富硅富碱、高铝富

钠、低钛、贫铁镁、强过铝质 ( $\text{A/CNK} > 1.30$ )，微量元素蛛网图呈左侧隆起、右侧平缓状，稀土元素配分曲线呈弱右倾的“海鸥型”，分异指数较高 ( $\text{DI} \geq 90$ )，表明其属强过铝质高分异 S 型花岗岩。

### 5.2.2 源区属性

形成伟晶岩（-细晶岩）的酸性岩浆一般是花岗质岩浆高程度结晶分异后的残余岩浆，上侵到浅部在半封闭或开放的条件下逐渐向富碱方向演化。花岗质岩浆高程度结晶分异以及晚阶段流体与熔体间交互作用使得 Nb 与 Ta、Zr 与 Hf 发生明显分馏，是稀有金属矿床形成的重要成矿机制（罗照华，

2011)。东槽含铌钽细晶岩属强过铝质高分异 S 型花岗岩,  $\text{CaO}/\text{Na}_2\text{O}$  值 ( $0.13\sim0.14$ )  $<0.30$ , 暗示其源区物质可能是富黏土矿物、贫斜长石的泥质岩。 $\text{Nb}/\text{Ta}$  值 ( $0.49\sim0.64$ ) 明显低于正常花岗岩的  $\text{Nb}/\text{Ta}$  值 (11),  $\text{Zr}/\text{Hf}$  值 ( $7.36\sim15.5$ ) 也低于正常花岗岩的  $\text{Zr}/\text{Hf}$  值 ( $33\sim40$ ) (Dostal and Chatterjee, 2000);  $\text{Rb}/\text{Sr}$  值 ( $24.6\sim165$ , 平均值为  $73.1$ ) 和  $\text{Rb}/\text{Nb}$  值 ( $11.9\sim16.4$ , 平均值为  $13.9$ ) 明显高于上地壳所对应的均值 (0.32 和 4.48), 表明该细晶岩岩浆源区物质可能是成熟度较高的上地壳富铝的变泥质岩石, 并且在岩浆演化过程中或者晚阶段发生了流体与熔体间的交互作用 (项新葵等, 2015; 李仁泽等, 2020)。结合岩石源区属性判别图解, 认为该细晶岩源岩可能是富黏土、富白云母的变泥质岩(图 8a、8b),

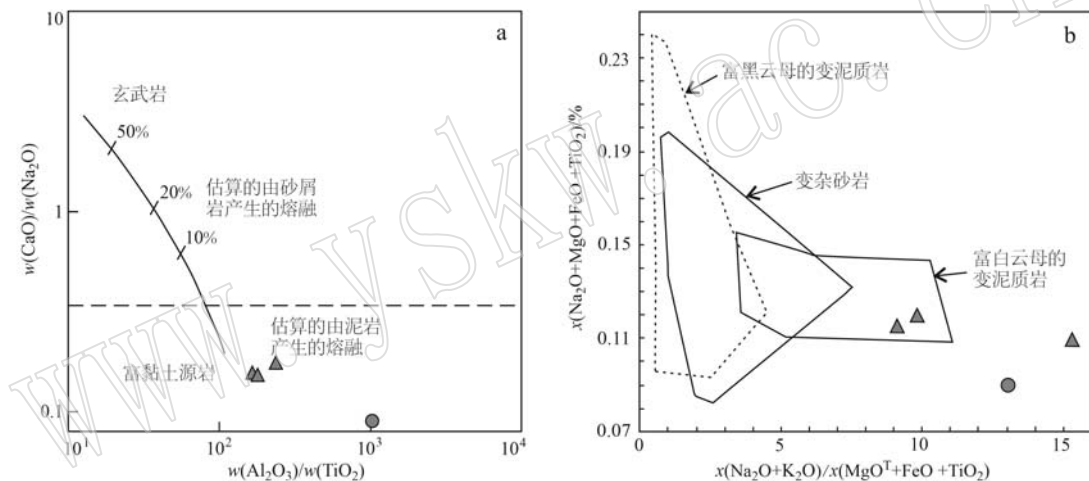


图 8 岩石源区属性判别图解

Fig. 8 Discrimination diagrams for the source characteristics

a— $\text{CaO}/\text{Na}_2\text{O}-\text{Al}_2\text{O}_3/\text{TiO}_2$  图 (底图据 Sylvester, 1998); b— $x(\text{Na}_2\text{O}+\text{MgO}+\text{FeO}+\text{TiO}_2)-x(\text{Na}_2\text{O}+\text{K}_2\text{O})/x(\text{MgO}^T+\text{FeO}+\text{TiO}_2)$

(底图据 Lee et al., 2003); 图例同图 6

a— $\text{CaO}/\text{Na}_2\text{O}-\text{Al}_2\text{O}_3/\text{TiO}_2$  diagram (schema from Sylvester, 1998); b— $x(\text{Na}_2\text{O}+\text{MgO}+\text{FeO}+\text{TiO}_2)-x(\text{Na}_2\text{O}+\text{K}_2\text{O})/x(\text{MgO}^T+\text{FeO}+\text{TiO}_2)$  diagram (schema from Lee et al., 2003); same symbols as in Fig. 6

东槽含铌钽细晶岩具有富铝、富碱、富集稀有金属 (Li、Rb、Cs、Ta、Nb、Be、Sn)、低的  $\text{Nb}/\text{Ta}$  值和  $\text{Zr}/\text{Hf}$  值, 起源于成熟地壳富铝的变泥质岩石, 形成于同碰撞向造山期后演变的挤压-伸展环境, 属强过铝质高分异 S 型花岗岩, 产有铌钽等稀有金属矿化, 归类于 LCT 型伟晶岩 (-细晶岩) (张辉等, 2021)。在系列花岗岩含矿性判别图解中, 东槽含铌钽细晶岩均落点于“南岭含铌钽花岗岩”区(图 9)。东槽含铌钽细晶岩与南岭含铌钽花岗岩、大湖塘含铌钽花岗斑岩的地球化学特征相似(表 3, 陈骏等, 2008; 刘莹等, 2018), 都富硅富铝低钛,  $\text{Al}_2\text{O}_3/\text{TiO}_2$ 、

与九岭地区新元古界双桥山群变泥质岩系相对应。

### 5.3 含铌钽细晶岩的找矿意义

华南地区多期构造-岩浆活动造成壳源物质循环, 使其成熟度不断增强, 造成 W、Sn、Nb、Ta、Li、Bi、U、REE 等元素在地壳不断富集(舒良树等, 2021)。变质基底中高的 W、Sn、Nb、Ta 等元素含量以及变沉积岩富集 Li、F、P 等元素, 是有色金属、稀有金属成矿的基础(马东升, 2008)。其中, 铌钽等稀有金属大规模成矿集中在燕山早期(晚侏罗世—早白垩世,  $140\text{ Ma}\pm$ )的“过渡阶段”(舒良树等, 2021)。九岭地区成熟度较高的中上地壳、燕山期强过铝质高分异 S 型花岗岩以及钠长石化、云英岩化、紫色萤石化、锂云母化等热液蚀变, 均是该区铌钽等稀有金属成矿的有利条件。

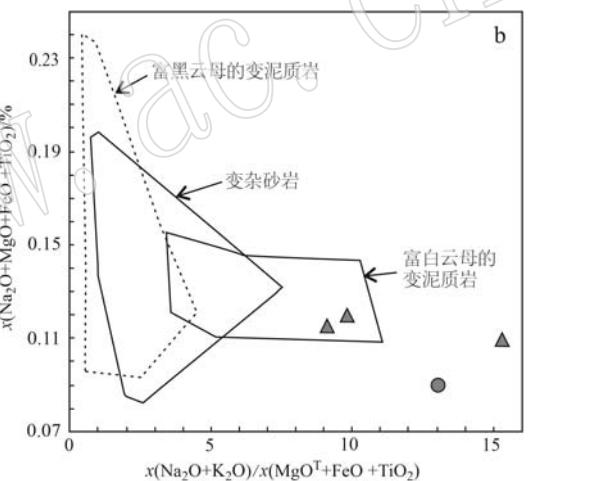


图 8 岩石源区属性判别图解

Fig. 8 Discrimination diagrams for the source characteristics

A/CNK  $> 1.1$ ,  $\text{CaO}/(\text{K}_2\text{O}+\text{Na}_2\text{O})$  比值低, 分异指数 DI 高,  $\text{Zr}+\text{Nb}+\text{Ce}+\text{Y}$  含量较低,  $\text{Rb}/\text{Sr}$  值高,  $\text{Zr}/\text{Hf}$  值、 $\text{Nb}/\text{Ta}$  值偏低, 明显富 Nb、Rb 和贫 Y、Ba+Sr, 稀土元素总量低, 轻重稀土元素比值较低, 明显负铕异常, 稀土元素配分曲线呈弱右倾的海鸥型, Nb 含量  $> 85\times10^{-6}$ 、Ta 含量  $> 155\times10^{-6}$ 、Li 含量  $> 1900\times10^{-6}$ , 这些是辨别花岗岩类岩石是否产有铌钽矿化的有益地球化学指标(表 3)。

燕山早期(晚侏罗世—早白垩世,  $152\sim128\text{ Ma}$ ), 九岭地区南部潭山-上富一带, 高硅富碱富铝的酸性岩浆沿 NNE 向走滑断裂上侵, 并在其与近东西向挤

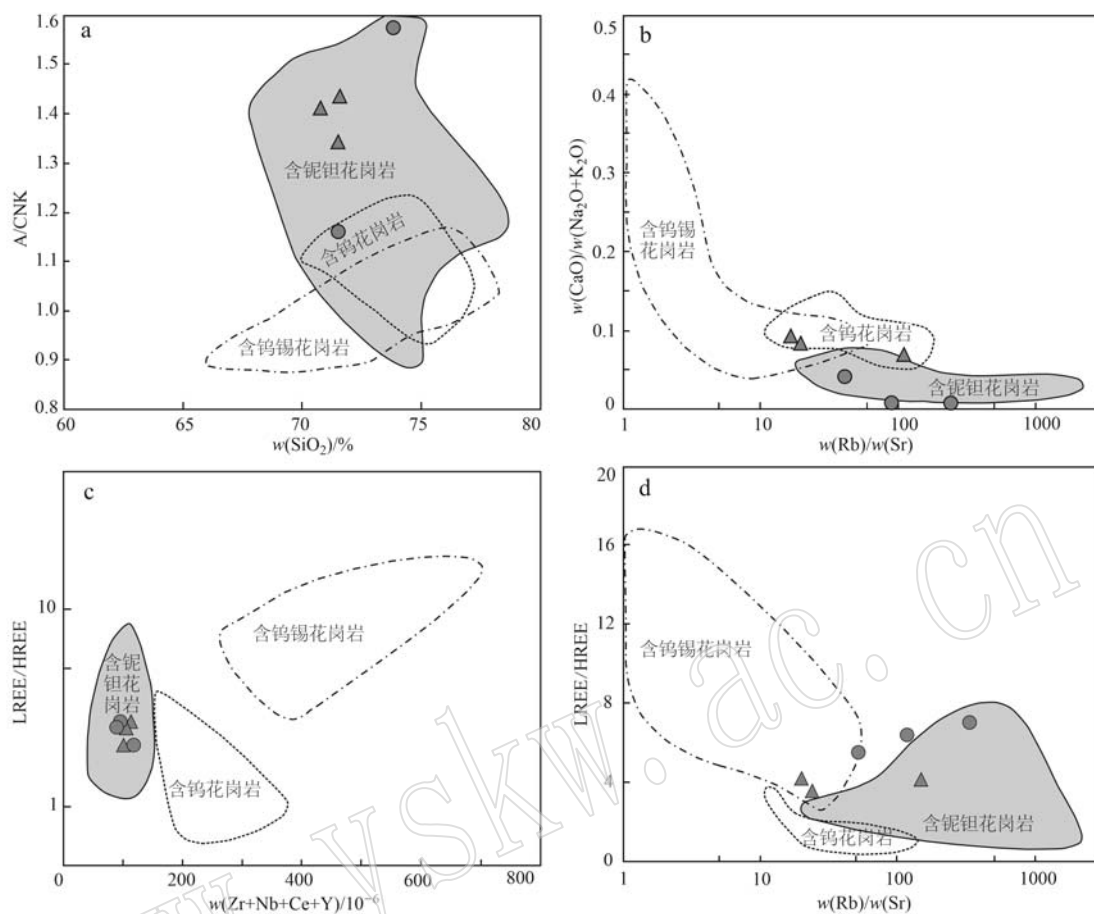


图9 不同类型含矿花岗岩判别图解(图例同图6)

Fig. 9 Discrimination diagrams for three types of ore-bearing granites (same symbols as in Fig. 6)

表3 含铌钽花岗岩主要地球化学指标  
Table 3 Main geochemical indicators for Nb-Ta-bearing granite

类比项目	东槽含铌钽细晶岩	大湖塘含铌钽花岗斑岩	南岭含铌钽花岗岩
SiO <sub>2</sub> /%	70.7~71.6>70.0	71.5~73.8>71.5	67.9~78.1>67.5
TiO <sub>2</sub> /%	0.07~0.10<0.10	0.02~0.04<0.10	0.01~0.09<0.10
Al <sub>2</sub> O <sub>3</sub> /%	16.2~16.8>16	16.1~16.7>16	-
Al <sub>2</sub> O <sub>3</sub> /TiO <sub>2</sub>	165~239>160	405~1073>400	152~1753, 均值705
(K <sub>2</sub> O+Na <sub>2</sub> O)%	7.13~7.85, 均值7.40	6.85~9.21, 均值7.86	5.49~10.6, 均值8.38
CaO/(K <sub>2</sub> O+Na <sub>2</sub> O)	0.07~0.10<0.10	0.01~0.04<0.10	0.02~0.12, 均值0.05
A/CNK	1.34~1.44>1.30	1.16~1.87>1.15	0.90~2.15, 均值1.23
ΣREE/10 <sup>-6</sup>	3.44~4.00, 均值3.73	7.10~19.0, 均值14.8	0.53~50.3, 均值19.1
LREE/HREE	2.82~3.60<4.00	4.77~6.30<8.00	1.15~7.77<8.00
δEu	0.10~0.29, 均值0.20	0.07~0.09, 均值0.08	0.02~0.42, 均值0.09
(Zr+Nb+Ce+Y)/10 <sup>-6</sup>	100~112<120	88.4~118, 均值100	49.8~144, 均值91.7
Li × 10 <sup>-6</sup>	1923~2630>1900	375~954>350	-
Nb × 10 <sup>-6</sup>	87.9~99.8>85	32.6~54.0>30	-
Ta × 10 <sup>-6</sup>	157~183>155	21.1~32.0>20	-
Rb/Sr	24.6~165, 平均73.1	61.0~361, 平均185	21.9~2017, 平均300
Nb/Ta	0.49~0.64, 平均0.56	1.44~1.69, 平均1.56	-
Zr/Hf	7.36~15.5, 平均10.5	11.6~12.5, 平均12.0	-
Nb <sub>2</sub> O <sub>5</sub> /%	0.010~0.019	-	-
Ta <sub>2</sub> O <sub>5</sub> /%	0.015~0.026	最高3.8	-
Li <sub>2</sub> O/%	0.100~0.800	最高2.1	-
数据来源	本文, 样品数3件	刘莹等, 2018; 褚平利等, 2019	陈骏等, 2008, 样品数为29件

压断裂交汇部位就位,形成细粒黑云母二长花岗岩、中细粒二云母二长花岗岩或白云母二长花岗岩,普遍发育钠长石化、锂云母化等自变质蚀变,派生(高程度结晶分异)出沿北东向、近东西向、北西向次级断裂充填的含铌钽的细晶岩脉、霏细斑岩脉、伟晶岩脉等(陈骏等,2008)。形成两类稀有金属矿化:一类以蚀变花岗岩型钽铌矿为主,铌钽矿化赋存于钠长石化白云母化细粒斑状黑云母二长花岗岩中,如大港、白市化山、白石里、狮子岭、白水洞、金港等矿床(吴学敏等,2016;秦程,2018;王成辉等,2019;李仁泽等,2020;汪炎炎等,2020;曾晓建等,2022;刘泽等,2023;Xu et al., 2023);一类以蚀变细晶岩和蚀变霏细斑岩为主,铌钽矿化赋存于斜长细晶岩和霏细斑岩中,如党田、茜坑、东槽等矿床(吴学敏等,2016;王成辉等,2018;谢军军等,2018;曾晓建等,2022)。这些稀有金属矿床共同组成了潭山-上富Nb-Ta-Li-Be成矿远景区。

综合分析认为,九岭地区燕山期NE向、近EW向斜长细晶岩、霏细斑岩、伟晶岩等脉岩均是寻找铌钽等稀有金属矿产的目标地质体,值得开展资源潜力调查。

## 6 结论

(1) 东槽细晶岩属强过铝质高分异S型花岗岩,形成于燕山早期(早白垩世),铌钽铁矿U-Pb年龄为 $142\pm1$  Ma;

(2) 东槽细晶岩具有富硅富碱富铝、低钛、低Ba-Sr、稀土元素总量低,明显负铕异常,Rb含量高,分异指数高、铌-钽-锂含量高等特征,与南岭含铌钽花岗岩、大湖塘含铌钽花岗斑岩特征相似;

(3) 东槽细晶岩推测为新元古界双桥山群变泥质岩发生部分熔融形成的花岗质岩浆,经历高程度分异结晶作用,并在岩浆演化晚阶段存在流体与熔体间的交互作用,最终形成沿NE向断裂呈脉状充填的斜长细晶岩脉。

(4) 东槽细晶岩发育钠长石化、白云母化、黄玉化、云英岩化等热液蚀变,氧化铌含量可达0.019%、氧化钽含量可达0.040%、氧化锂含量可达0.800%,是在潭山-上富成矿远景区内寻找铌钽矿床的目标地质体。

## References

- Che X D, Wu F Y, Wang R C, et al. 2015. In situ U-Pb isotopic dating of columbite-tantalite by LA-ICP-MS [J]. Ore Geology Reviews, 65(4): 979~989.
- Che X D, Wang R C, Wu F Y, et al. 2019. Episodic Nb-Ta mineralisation in South China: Constraints from in situ LA-ICP-MS columbite-tantalite U-Pb dating [J]. Ore Geology Reviews, 105: 71~85.
- Chen Jun, Lu Jianjun, Chen Weifeng, et al. 2008. W-Sn-Nb-Ta-bearing granites in the Nanling range and their relationship to metallogeny [J]. Geological Journal of China Universities, 14(4): 459~473 (in Chinese with English abstract).
- Chen Maosong, Xiang Xinkui, Zhan Gangjie, et al. 2020. Geochronology, geochemical characteristics of the post-mineralization Late Yan-shanian granite porphyry and its constraints for the terminal of the metallogeny in the No. 1 ore belt of the Dahutang district [J]. Journal of East China University of Technology (Natural Science), 43(5): 401~416 (in Chinese with English abstract).
- Chu Pingli, Duan Zheng, Liao Shengbing, et al. 2019. Petrogenesis and tectonic significances of Late Mesozoic granitoids in the Dahutang area, Jiangxi Province: Constraints from zircon U-Pb dating, mineral-chemistry, geochemistry and Hf isotope [J]. Acta Geologica Sinica, 93(7): 1 687~1 707 (in Chinese with English abstract).
- Dostal J and Chatterjee A K. 2000. Contrasting behaviour of Nb/Ta and Zr/Hf ratios in a peraluminous granitic pluton (Nova Scotia, Canada) [J]. Chemical Geology, 163(1~4): 207~218.
- Duan Zheng, Liao Shengbing, Chu Pingli, et al. 2019. Zircon U-Pb ages of the Neoproterozoic Jiuling complex granitoid in the eastern segment of the Jiangnan orogen and its tectonic significance [J]. Geology in China, 46(3): 493~516 (in Chinese with English abstract).
- Feng Chengyou, Zhang Dequan, Xiang Xinkui, et al. 2012. Re-Os isotopic dating of molybdenite from the Dahutang tungsten deposit in northwestern Jiangxi Province and its geological implication [J]. Acta Petrologica Sinica, 28(12): 3 858~3 868 (in Chinese with English abstract).
- Frost B R, Barnes C G and Collins W J. 2001. A geochemical classification for granitic rocks [J]. Journal of Petrology, 42(11): 2 033~2 048.

- Gao S, Liu X M, Yuan H L, et al. 2002. Determination of forty two major and trace elements in USGS and NIST SRM glasses by laser ablation inductively coupled plasma mass spectrometry geostandards [J]. *News Letter Journal of Geostandards and Geoanalysis*, 26: 191~196.
- Huang Lanchun and Jiang Shaoyong. 2012. Zircon U-Pb geochronology, geochemistry and petrogenesis of the porphyric-like muscovite granite in the Dahutang tungsten deposit, Jiangxi Province [J]. *Acta Petrologica Sinica*, 28(12): 3 887~3 900 (in Chinese with English abstract).
- Huang Lanchun and Jiang Shaoyong. 2013. Geochronology, geochemistry and petrogenesis of the tungsten-bearing porphyritic granite in the Dahutang tungsten deposit, Jiangxi Province [J]. *Acta Petrologica Sinica*, 29(12): 4 323~4 335 (in Chinese with English abstract).
- Jiang Shaoyong, Peng Ningjun, Huang Lanchun, et al. 2015. Geological characteristic and ore genesis of the giant tungsten deposits from the Dahutang ore-concentrated district in northern Jiangxi Province [J]. *Acta Petrologica Sinica*, 31(3): 639~655 (in Chinese with English abstract).
- Lee S Y, Barnes C G, Snook A W, et al. 2003. Petrogenesis of mesozoic, peraluminous granites in the lamoille canyon area, ruby mountains, Nevada, USA [J]. *Journal of Petrology*, 44(4): 713~732.
- Li Hang, Hong Tao, Yang Zhiqian, et al. 2020. Comparative studying on zircon, cassiterite and columbite U-Pb dating and  $^{40}\text{Ar}/^{39}\text{Ar}$  dating of muscovite rare-metal granitic pegmatites: A case study of the northern Tugeman lithium-beryllium deposit in the middle of Altyn Tagh [J]. *Acta Petrologica Sinica*, 36(9): 2 869~2 892 (in Chinese with English abstract).
- Li Wufu, Liu Jinheng, Li Shanping, et al. 2022. Discovery and mineralization significance of Early Jurassic (beryl- and lepidolite-) spodumene-bearing pegmatites in the Gaduo-Zaduo area of the Yushu region, northeastern Tibet [J]. *Geotectonica et Metallogenesis*, 46(5): 924~950 (in Chinese with English abstract).
- Li Renze, Zhou Zhengbing, Peng Bo, et al. 2020. A discussion on geological characteristics and genetic mechanism of Dagang superlarge lithium-bearing porcelain stone deposit in Yifeng County, Jiangxi Province [J]. *Mineral Deposits*, 39(6): 1 015~1 029 (in Chinese with English abstract).
- Linnen R L and Keppler H. 2002. Melt composition control of Zr/Hf fractionation in magmatic processes [J]. *Geochimica et Cosmochimica Acta*, 66(18): 3 293~3 301.
- Liu Xinxing, Zhang Juan, Li Xiaolong, et al. 2023. Metallogeny of the Longtangou-Huoyangou Sn deposit in North Qinling Orogeny: Geochronological and petrogeochemical evidence from Sn-bearing granite-pegmatite [J]. *Acta Petrologica Sinica*, 39(5): 1 484~1 500 (in Chinese with English abstract).
- Liu Ying, Xie Lei, Wang Rucheng, et al. 2018. Comparative study of petrogenesis and mineralization characteristics of Nb-Ta- bearing and W-bearing granite in the Dahutang deposit, northern Jiangxi Province [J]. *Acta Geologica Sinica*, 92(10): 2 120~2 137 (in Chinese with English abstract).
- Liu Y S, Hu Z C, Zong K Q, et al. 2010. Reappraisal and refinement of zircon U-Pb isotope and trace element analyses by LA-ICP-MS [J]. *Chinese Science Bulletin*, 55(15): 1 535~1 546.
- Liu Ze, Chen Zhenyu, Wang Chenghui, et al. 2023. Mineralogical characteristics and metallogenic mechanism of Shiziling Li-Ta deposit in Northwest Jiangxi [J]. *Acta Petrologica Sinica*, 39(7): 2 045~2 062 (in Chinese with English abstract).
- Ludwig K R. 2003. User's manual for Isoplot/Ex, Version 3.00. A geochronological toolkit for Microsoft excel [J]. Berkeley Geochronology Center Special Publication, 4(2): 1~70.
- Luo Zhaohua. 2011. The metallogenic function of fluid-melt strong interaction [J]. *Acta Mineralogica Sinica*, 31(S1): 503~504 (in Chinese).
- Lü Shujun, Dong Guochen, Luo Zhibo, et al. 2023. Lithium mineralization characteristics and chronology of spodumene granite pegmatite in the northern Chaka Mountain, Qinghai Province [J]. *Acta Petrologica et Mineralogica*, 42(3): 350~364 (in Chinese with English abstract).
- Ma Dongsheng. 2008. Metallogenetic characteristics of the important deposits in South China [J]. *Bulletin of Mineralogy, Petrology and Geochemistry*, 27(3): 209~217 (in Chinese with English abstract).
- Maniar P D and Piccoli P M. 1989. Tectonic discrimination of granitoid [J]. *Geological Society of America Bulletin*, 101(5): 635~643.
- Mao Jingwen, Chen Maohong, Yuan Shunda, et al. 2011. Characteristics and spatial-temporal regularity of mineral deposits in Qinhang (or Shihang) metallogenic belt, South China [J]. *Acta Geologica Sinica*, 85(5): 636~658 (in Chinese with English abstract).
- Middlemost E A K. 1994. Naming materials in the magma/igneous rock system [J]. *Annual Review of Earth & Planetary Sciences*, 37(3~4): 215~224.
- Pearce N J G, Perkins W T, Westgate J A, et al. 1997. A compilation of

- new and published major and trace element data for NIST SRM 610 and NIST SRM 612 glass reference materials [J]. *Geostandards and Geoanalytical Research*, 21(1): 115~144.
- Peccerillo A and Taylor S R. 1976. Geochemistry of Eocene calc-alkaline volcanic rocks from the Kastamonu area, Northern Turkey [J]. *Contributions to Mineralogy and Petrology*, 58(1): 63~81.
- Peng Huaming, Xia Fei, Yan Zhaobin, et al. 2014. Features, genesis and geological significance of zircons from the granite porphyry in the Dalingshang tungsten deposit, Jiangxi Province [J]. *Acta Petrologica et Mineralogica*, 33(5): 811~824 (in Chinese with English abstract).
- Qin Cheng. 2018. Preliminary Study of Mineralization Potentiality of Shiziling Muscovite Granite, Jiangxi Province [D]. Beijing: China University of Geosciences (Beijing) (in Chinese with English abstract).
- Shu Liangshu, Zhu Wenbin, Xu Zhiqin, et al. 2021. Geological settings and metallogenetic conditions of the granite-type lithium ore deposits in South China [J]. *Acta Geologica Sinica*, 95(10): 3 099~3 114 (in Chinese with English abstract).
- Sun S S and McDonough W F. 1989. Chemical and isotopic systematics of oceanic basalts: Implications for mantle composition and processes [J]. *Geological Society of London, Special Publications*, 42(1): 313~345.
- Sylvester P J. 1998. Post-collisional strongly peraluminous granites [J]. *Lithos*, 45(1~4): 29~44.
- Wang Chenghui, Wang Denghong, Chen Chen, et al. 2021. Progress of research on the Shilizing rare metals mineralization from Jiuling-type rock and its significance for prospecting [J]. *Acta Geologica Sinica*, 93(6): 1 359~1 373 (in Chinese with English abstract).
- Wang Di. 2017. Formation of Huge Composite Granitic Batholiths in Jiuling area of north Jiangxi Province [D]. Beijing: Nanjing University (in Chinese with English abstract).
- Wang He, Gao Hao, Wang Saimeng, et al. 2022. Zircon and columbite-tantalite U-Pb geochronology of Li-Be rare metal pegmatite and its geological significance in Muji area, West Kunlun, China [J]. *Acta Petrologica Sinica*, 38(7): 1 937~1 951 (in Chinese with English abstract).
- Wang Jinrong, Lü Zhenghang, Lü Xinbiao, et al. 2020. LA-ICP-MS U-Pb age of columbite from the Daping granite porphyry-type rare metal deposit in Fujian Province and its geological significance [J]. *Bulletin of Mineralogy, Petrology and Geochemistry*, 39(3): 637~645 (in Chinese with English abstract).
- Wang Yanyan and Ouyang Zhigang. 2020. Metallogenetic characteristics and prospecting potential of lithium and rare metals in BaiShiLi mining area, Yifeng County, Jiangxi Province [J]. *World Nonferrous Metals*, (1): 66~67 (in Chinese with English abstract).
- Whalen J B, Currie K L and Chappell B W. 1987. A-type granites: Geochemical characteristics, discrimination and petrogenesis [J]. *Contributions to Mineralogy and Petrology*, 95(4): 407~419.
- Wu Xuemin, Zhou Minjuan, Luo Xicheng, et al. 2016. The metallogenetic conditions and prospecting potential of lithium and rare metals in northwestern Jiangxi [J]. *East China Geology*, 37(4): 275~283 (in Chinese with English abstract).
- Wu Xianyuan, Zhang Zhiyu, Zheng Yuanchuan, et al. 2019. Magmatism, genesis and significance of multi-stage porphyry-like granite in the giant Dahutang tungsten deposit, northern Jiangxi Province [J]. *Acta Petrologica et Mineralogica*, 38(3): 318~338 (in Chinese with English abstract).
- Wright J B. 1969. A simple alkalinity ratio and its application to questions of non-orogenic granite genesis [J]. *Geological Magazine*, 106(4): 370~384.
- Xiang Xinkui, Yin Qingqing, Sun Keke, et al. 2015. Origin of the Dahutang syn-collisional granite-porphyry in the middle segment of the Jiangnan orogen: Zircon U-Pb geochronologic, geochemical and Nd-Hf isotopic constraints [J]. *Acta Petrologica et Mineralogica*, 34(5): 581~600 (in Chinese with English abstract).
- Xie Junjun and Yang Li. 2018. Characteristics of rare metal resources such as lithium in Yifeng area [J]. *World Nonferrous Metals*, (21): 94, 97 (in Chinese with English abstract).
- Xu Z, Zhang Y, Pan J Y, et al. 2023. In situ LA-ICP-MS analyses of muscovite: Constraints on granite-type Li mineralization in northwestern Jiangxi, South China [J]. *Ore Geology Reviews*, 156: 105402.
- Yang Mingui, Wang Faning, Zeng Yong, et al. 2004. Metallogenetic Geology of Northern Jiangxi [M]. China Land Press (Beijing) (in Chinese).
- Zeng Xiaojian, Liu Jianwei, Zeng Qingyou, et al. 2022. Geochemical characteristics and genesis of the proclain stone (lithium-bearing) in Yifeng area, Jiangxi Province [J]. *Nonferrous Metals (Mining Section)*, 74(4): 128~136 (in Chinese with English abstract).
- Zhang Hui, Lü Zhenghang and Tang Yong. 2021. A review of LCT pegmatite and its lithium ore genesis [J]. *Acta Geologica Sinica*, 95(10): 2 955~2 970 (in Chinese with English abstract).
- Zhang Yong. 2018. Ore-forming Fluid Evolution and Sb-Au-W Metallogenetic characteristics and prospecting potential of lithium and rare metals in BaiShiLi mining area, Yifeng County, Jiangxi Province [J]. *World Nonferrous Metals*, (1): 66~67 (in Chinese with English abstract).

- genesis in the Central Hunan-Northwestern Jiangxi, South China [D]. Nanjing: Nanjing University (in Chinese with English abstract).
- Zhang Yong, Pan Jiayong, Ma Dongsheng, et al. 2017. Re-Os molybdenite age of Dawutang tungsten ore district of northwest Jiangxi and its geological significance [J]. Mineral Deposits, 36(3): 749~769 (in Chinese with English abstract).
- Zhang Yong, Pan Jiayong, Ma Dongsheng, et al. 2020. Lithium element enrichment and inspiration for prospecting for rare-metal mineralization in the Dahutang tungsten deposit: Constraints from mineralogy and geochemistry of hydrothermal alteration [J]. Acta Geologica Sinica, 94(11): 3 321~3 342 (in Chinese with English abstract).
- Zhao Zheng, Chen Yuchuan, Wang Denghong, et al. 2022. Transformation of Mesozoic dynamic systems and superposition of metallogenetic series of W-Sn-Li-Be-Nb-Ta-REE mineral deposits in South China [J]. Acta Petrologica Sinica, 38(2): 301~322 (in Chinese with English abstract).
- Zhong Long, Wang Zhenghua, Liu Yulin, et al. 2011. The geochronology research status of Altal pegmatite, NW China: The confusion of the conventional dating methods used in granitic pegmatite [J]. Xinjiang Geology, 29(4): 412~415 (in Chinese with English abstract).
- 附中文参考文献
- 陈 骏, 陆建军, 陈卫锋, 等. 2008. 南岭地区钨锡铌钽花岗岩及其成矿作用 [J]. 高校地质学报, 14(4): 459~473.
- 陈茂松, 项新葵, 占岗乐, 等. 2020. 大湖塘矿集区一矿带燕山晚期成矿后花岗斑岩年代学、地球化学特征及对成矿结束时间的约束 [J]. 东华理工大学学报(自然科学版), 43(5): 401~416.
- 褚平利, 段 政, 廖圣兵, 等. 2019. 江西大湖塘中生代花岗岩的成因与构造指示意义: 年代学、矿物化学、地球化学与 Lu-Hf 同位素制约 [J]. 地质学报, 93(7): 1 687~1 707.
- 段 政, 廖圣兵, 褚平利, 等. 2019. 江南造山带东段新元古代九岭复式岩体锆石 U-Pb 年代学及构造意义 [J]. 中国地质, 46(3): 493~516.
- 丰成友, 张德全, 项新葵, 等. 2012. 赣西北大湖塘钨矿床辉钼矿 Re-Os 同位素定年及其意义 [J]. 岩石学报, 28(12): 3 858~3 868.
- 黄兰椿, 蒋少涌. 2012. 江西大湖塘钨矿床似斑状白云母花岗岩锆石 U-Pb 年代学、地球化学及成因研究 [J]. 岩石学报, 28(12): 3 887~3 900.
- 黄兰椿, 蒋少涌. 2013. 江西大湖塘富钨花岗岩年代学、地球化学特征及成因研究 [J]. 岩石学报, 29(12): 4 323~4 335.
- 蒋少涌, 彭宁俊, 黄兰椿, 等. 2015. 赣北大湖塘矿集区超大型钨矿地质特征及成因探讨 [J]. 岩石学报, 31(3): 639~655.
- 李 杭, 洪 涛, 杨智全, 等. 2020. 稀有金属花岗伟晶岩锆石、锡石与铌钽铁矿 U-Pb 和白云母<sup>40</sup>Ar/<sup>39</sup>Ar 测年对比研究——以阿尔金中段吐格曼北锂铍矿床为例 [J]. 岩石学报, 36(9): 2 869~2 892.
- 李仁泽, 周正兵, 彭 波, 等. 2020. 江西宜丰县大港超大型含锂瓷石矿床地质特征及成因机制探讨 [J]. 矿床地质, 39(6): 1 015~1 029.
- 李五福, 刘金恒, 李善平, 等. 2022. 青藏高原东北部玉树地区尕朵-扎朵早侏罗世含(绿柱石-锂云母)锂辉石伟晶岩的发现及成矿意义 [J]. 大地构造与成矿学, 46(5): 924~950.
- 刘新星, 张 娟, 李肖龙, 等. 2023. 北秦岭卢氏龙潭沟-火炎沟锡矿床成矿作用探讨——来自花岗伟晶岩年代学、岩石地球化学的证据 [J]. 岩石学报, 39(5): 1 484~1 500.
- 刘 莹, 谢 磊, 王汝成, 等. 2018. 赣北大湖塘矿床的含铌钽与含钨花岗岩成岩成矿特征对比研究 [J]. 地质学报, 92(10): 2 120~2 137.
- 刘 泽, 陈振宇, 王成辉. 2023. 赣西北狮子岭花岗岩型锂-钽矿床的矿物学特征及成矿机制 [J]. 岩石学报, 39(7): 2 045~2 062.
- 罗照华. 2011. 流体-熔体强相互作用的成矿功能 [J]. 矿物学报, 31(S1): 503~504.
- 吕书俊, 董国臣, 罗志波, 等. 2023. 茶卡北山锂辉石花岗伟晶岩锂矿化特征及成矿时限 [J]. 岩石矿物学杂志, 42(3): 350~364.
- 马东升. 2008. 华南重要金属矿床的成矿规律——时代爆发性、空间分带性、基底继承性和热隆起成矿 [J]. 矿物岩石地球化学通报, 27(3): 209~217.
- 毛景文, 陈懋弘, 袁顺达, 等. 2011. 华南地区钦杭成矿带地质特征和矿床时空分布规律 [J]. 地质学报, 85(5): 636~658.
- 彭花明, 夏 菲, 严兆彬, 等. 2014. 江西大岭上钨矿花岗斑岩锆石特征、成因及意义 [J]. 岩石矿物学杂志, 33(5): 811~824.
- 秦 程. 2018. 江西宜丰狮子岭白云母花岗岩成矿潜力研究 [D]. 北京: 中国地质大学(北京).
- 舒良树, 朱文斌, 许志琴, 等. 2021. 华南花岗岩型锂矿地质背景与成矿条件 [J]. 地质学报, 95(10): 3 099~3 114.
- 王成辉, 王登红, 陈 晨, 等. 2019. 九岭式狮子岭岩体型稀有金属成矿作用研究进展及其找矿意义 [J]. 地质学报, 93(6): 1 359~1 373.
- 王 迪. 2017. 赣北九岭地区巨型复式花岗岩基的形成 [D]. 南京:

- 南京大学.
- 王核,高昊,王赛蒙,等.2022.新疆西昆仑木吉地区锂铍稀有金属伟晶岩锆石及铌钽铁矿U-Pb年代学、Hf同位素组成及其地质意义[J].岩石学报,38(7):1937~1951.
- 王锦荣,吕正航,吕新彪,等.2020.福建大坪花岗斑岩型稀有金属矿床铌铁矿LA-ICP-MS U-Pb定年及其地质意义[J].矿物岩石地球化学通报,39(3):637~645.
- 汪炎炎,欧阳志刚.2020.江西省宜丰县白石里矿区锂及稀有金属成矿特征及找矿潜力分析[J].世界有色金属,(1):66~67.
- 吴显愿,张智宇,郑远川,等.2019.赣北大湖塘超大型钨矿多期似斑状花岗岩岩浆作用、成因及意义[J].岩石矿物学杂志,38(3):318~338.
- 吴学敏,周敏娟,罗喜成,等.2016.江西西北部锂及稀有金属成矿条件及找矿潜力分析[J].华东地质,37(4):275~283.
- 项新葵,尹青青,孙克克,等.2015.江南造山带中段大湖塘同构造花岗斑岩的成因——锆石U-Pb年代学、地球化学和Nd-Hf同位素制约[J].岩石矿物学杂志,34(5):581~600.
- 谢军军,杨莉.2018.宜丰地区含锂等稀有金属矿资源特征[J].世界有色金属,(21):94,97.
- 杨明桂,王发宁,曾勇,等.2004.江西北部金属成矿地质[M],北京:中国大地出版社.
- 曾晓建,刘建伟,曾庆友,等.2022.江西宜丰地区瓷石矿(含锂)地球化学特征及成因[J].有色金属(矿山部分),74(4):128~136.
- 张辉,吕正航,唐勇.2021.LCT型伟晶岩及其锂矿床成因概述[J].地质学报,95(10):2955~2970.
- 张勇.2018.湘中-赣西北成矿流体演化与Sb-Au-W成矿[D].南京:南京大学.
- 张勇,潘家永,马东升,等.2017.赣西北大雾塘钨矿区地质特征及Re-Os同位素年代学研究[J].矿床地质,36(3):749~769.
- 张勇,潘家永,马东升.2020.赣西北大湖塘钨矿富锂-云母化岩锂元素富集机制及其对锂等稀有金属找矿的启示[J].地质学报,94(11):3321~3342.
- 赵正,陈毓川,王登红,等.2022.华南中生代动力体制转换与钨锡锂铍铌钽稀土矿床成矿系列的叠加演化[J].岩石学报,38(2):301~322.
- 钟龙,王政华,刘玉琳.2011.阿尔泰花岗伟晶岩年代学研究现状——兼谈常规年代学方法在花岗伟晶岩定年中之困惑[J].新疆地质,29(4):412~415.